MIMO OFDM Receivers for Systems With IQ Imbalances

Alireza Tarighat, *Student Member, IEEE,* and Ali H. Sayed, *Fellow, IEEE*

***Abstract*—Orthogonal frequency division multiplexing (OFDM) is a widely recognized modulation scheme for high data rate communications. However, the implementation of OFDM-based systems suffers from in-phase and quadrature-phase (IQ) imbalances in the front-end analog processing. Such imbalances are caused by the analog processing of the received radio frequency (RF) signal, and they cannot be efficiently or entirely eliminated in the analog domain. The resulting IQ distortion limits the achievable operating SNR at the receiver and, consequently, the achievable data rates. The issue of IQ imbalances is even more severe at higher SNR and higher carrier frequencies. In this paper, the effect of IQ imbalances on multi-input multioutput (MIMO) OFDM systems is studied, and a framework for combating such distortions through digital signal processing is developed. An input–output relation governing MIMO OFDM systems is derived. The framework is used to design receiver algorithms with compensation for IQ imbalances. It is shown that the complexity of the system at the receiver grows from dimension $(n_R \times n_T)$ for ideal IQ branches to $(2n_R \times 2n_T)$ in the presence of IQ imbalances. However, by exploiting the structure of space-time block codes along with the distortion models, one can obtain efficient receivers that are robust to IQ imbalances. Simulation results show significant improvement in the achievable BER of the proposed MIMO receivers for space-time block-coded OFDM systems in the presence of IQ imbalances.**

***Index Terms*—Alamouti scheme, compensation algorithms for analog impairments, in-phase and quadrature-phase (IQ) imbalances, multi-input multioutput (MIMO) systems, orthogonal frequency division multiplexing (OFDM), space-time coding.**

I. Introduction

ORTHOGONAL frequency division multiplexing (OFDM) is a widely adopted modulation technique for high-speed wireless communications. The OFDM-based physical layer has been chosen for several standards, such as the IEEE 802.11a wireless local area network (WLAN) in the 5-GHz band, the IEEE 802.11g wireless local area network (WLAN) in the 2.4 GHz band, and the European digital video broadcasting system (DVB-T). It is also under consideration as the high rate alternate physical layer to the draft IEEE P802.15.3 wireless personal area network (WPAN), the IEEE 802.20 mobile broadband wireless access (MBWA), and the IEEE 802.16 wireless metropolitan area networks (WirelessMAN). Considering the large demand for such systems, a low-cost, low-power, and fully integrated implementation of these standards is a challenge for the future high-speed wireless networks.

One limiting issue in implementing wireless systems is the impairment associated with analog processing due to component imperfections. The impairment in the analog components is mainly due to fabrication process variations, which are neither predictable nor controllable, and tend to increase as the fabrication technologies scale down [2]. Most of the impairments can be neither efficiently nor entirely eliminated in the analog domain due to power-area-cost tradeoffs. Therefore, an efficient compensation scheme in the digital baseband domain would be highly desirable for wireless receivers.

A major source of impairments in wireless system implementation is the imbalance between the In-phase (I) and Quadrature-phase (Q) branches or, equivalently, the real and imaginary parts of the complex signal, as explained in [4]. The IQ imbalance is basically any mismatch between the I and Q branches from the ideal case, i.e., from the exact 90° phase difference and equal amplitudes between the sine and cosine branches [5]. The performance of a receiver can be severely limited by such IQ imbalances.[1]

The approach developed in this paper for compensating IQ imbalances extends the method of [4] from the SISO case to MIMO systems. The motivation for the approach is as follows. 1) Perfect IQ matching is not possible in the analog domain, especially when low-cost fabrication technologies are used [6]. 2) As the carrier frequencies increase, the IQ imbalances become more severe and more challenging to eliminate. The increase in carrier frequencies translates to higher IQ imbalances, and the trend in communications systems is to utilize more bandwidth and higher carrier frequencies. 3) The impairments in analog processing tend to increase as integrated circuit technologies, such as complementary metal-oxide semiconductor (CMOS) technology, are being more widely adopted for analog processing due to their cost advantage and ease of integration with digital baseband processing [4]. 4) Efficient techniques can be developed in the digital domain to eliminate mismatches introduced in the analog domain. Note that such mismatches vary from chip to chip and are not predictable. 5) As higher data rates are targeted, higher constellation sizes are needed, and higher operating SNRs are to be guaranteed in order to support high density constellations.

Manuscript received March 31, 2004; revised September 19, 2004. This work was supported in part by the National Science Foundation under Grants CCF-0208573 and ECS-0401188. Part of this work was presented at the IEEE Sensor Array and Multichannel Signal Processing Workshop (SAM), 2004 [1]. The associate editor coordinating the review of this manuscript and approving it for publication was Dr. Athina Petropulu.

The authors are with the Department of Electrical Engineering, University of California, Los Angeles, CA 90095 USA (e-mail: tarighat@ee.ucla.edu; bagheri@ee.ucla.edu; sayed@ee.ucla.edu).

Digital Object Identifier 10.1109/TSP.2005.853148

[1]To avoid lengthy circuit implementation details, only the IQ imbalance in the down-conversion stage has been described here as a source of IQ imbalance. However, there are other analog processing stages that contribute to the overall IQ imbalance in the system. For instance, any mismatch between the frequency responses of the analog passband and lowpass filters used in the I and Q branches contribute to the overall IQ imbalances in the receiver. In this case, the distortion will have a frequency-dependent nature; see Section VII-A.

Higher SNR requirements translate to tougher IQ matching requirements. 6) MIMO systems can provide higher effective SNR and, consequently, higher data throughput by enabling higher density constellations. At high SNR values, however, the BER performance of the system is more severely affected by IQ imbalances, requiring some type of compensation. Likewise, the gain achieved by space-time coded MIMO systems compared to SISO systems is more significant at high SNR values.

For all the above reasons, it is desirable to develop reception techniques in the digital domain that help eliminate the effect of IQ imbalances in wireless receivers. The effect of IQ imbalances on SISO OFDM systems and the resulting performance degradation have already been investigated in [7] and [8]. Several compensation schemes have been developed in [3] and [9]–[11]. However, studying the effect of IQ imbalances on MIMO OFDM systems is more demanding. The purpose of this paper is to study the effect of IQ imbalances on MIMO systems and to develop a framework to design MIMO receiver architectures that are robust to IQ imbalances. The contribution of the paper is twofold. First, the input–output relation governing MIMO OFDM systems with IQ imbalances is derived. This relation is derived as a function of MIMO channel and physical parameters modeling IQ imbalances. It is shown that the system of equations governing the input–output relation for uncoded MIMO OFDM systems with IQ imbalances extends from dimension $(n_R \times n_T)$ in the case of ideal IQ branches to $(2n_R \times 2n_T)$ in the presence of IQ imbalances. Here, n_R and n_T denote the number of receive and transmit antennas, respectively. Second, the behavior of space-time block coded systems in the presence of IQ imbalances is studied. By exploiting the structure of orthogonal space-time codes, efficient receiver architectures that are robust to IQ imbalances are derived. They achieve a performance close to ideal receivers. In particular, a receiver architecture is proposed for Alamouti-coded OFDM systems with compensation for IQ imbalances. The proposed scheme is further extended to other orthogonal space-time block codes. It is shown how the code structure and the distortion model can be exploited in the design of efficient and optimal receivers.

The paper is organized as follows. Section II briefly describes the model used for IQ imbalances and formulates the effect of IQ imbalances on SISO OFDM receivers. In Section III, the formulation is used to develop a framework and to study the effect of IQ imbalances on MIMO OFDM systems. Space-time block-coded MIMO systems with imbalances are studied in Section IV. An efficient receiver for an Alamouti-coded OFDM system with compensation for IQ imbalances is proposed in Section V. The receiver architecture is extended to other orthogonal space-time block codes in Section VI. Some issues regarding the channel/distortoion estimation and frequency-selectivity of imbalances are addressed in Section VII. Simulation results are presented in Section VIII. Conclusions are given in Section IX.

Notation: All matrices are denoted in capital boldface letters.

II. Problem Formulation for SISO OFDM Systems

We review, in this section, the formulation of [3] in preparation for the extention to the MIMO case. Thus, let $b(t)$ represent the received complex signal before being distorted by the IQ imbalance caused by the analog signal processing. The distorted signal in the time domain can be modeled as [7], [8]

$$b'(t) = \mu b(t) + \nu b^*(t) \tag{1}$$

where the distortion parameters μ and ν are related to the amplitude and phase imbalances between the I and Q branches in the RF/Analog demodulation process. A simplified model for this distortion, assuming an amplitude imbalance and a phase imbalance between the I and Q branches of the mixer, can be derived. For such a case, the μ and ν parameters can be written as [8]

$$\begin{aligned} \mu &= \cos\left(\frac{\theta}{2}\right) + j\alpha \sin\left(\frac{\theta}{2}\right) \\ \nu &= \alpha \cos\left(\frac{\theta}{2}\right) - j \sin\left(\frac{\theta}{2}\right) \end{aligned} \tag{2}$$

where θ and α are, respectively, the phase and amplitude imbalance between the I and Q branches. The phase imbalance is any phase deviation from the ideal 90° between the I and Q branches. The amplitude imbalance is defined as

$$\alpha = \frac{a_I - a_Q}{a_I + a_Q}$$

where a_I and a_Q are the gain amplitudes on the I and Q branches. When stated in decibels, the amplitude imbalance is computed as $10\log(1+\alpha)$. For instance, an amplitude imbalance of 0 dB corresponds to the ideal case of $\alpha = 0$. The values of θ and α are not known at the receiver since they are caused by manufacturing inaccuracies in the analog components.

The effect of IQ imbalances on an SISO OFDM system has been discussed in [9]–[11]. A derivation of the OFDM signals in the presence of IQ imbalances using the formulation of and [3] is reviewed below. This formulation will help us extend the results to the MIMO case.

In OFDM systems, a block of data is transmitted as an OFDM symbol. Assuming a block size equal to N (where N is a power of 2), the transmitted block of data is denoted by

$$\mathbf{s} \triangleq \text{col}\{\mathbf{s}(1), \mathbf{s}(2), \ldots, \mathbf{s}(N)\}. \tag{3}$$

Each block is passed through the IDFT operation

$$\bar{\mathbf{s}} = \mathbf{F}^* \mathbf{s} \tag{4}$$

where $\mathbf{F}$ is the unitary discrete Fourier transform (DFT) matrix of size N, which is defined by

$$[\mathbf{F}]_{ik} \triangleq \frac{1}{\sqrt{N}} \exp \frac{-j2\pi ik}{N}, \quad j = \sqrt{-1}$$
$$i,k = \{0, 1, \ldots, N-1\}.$$

A cyclic prefix of length P is added to each transformed block of data and then transmitted through the channel; see Fig. 1. An FIR model with $L+1$ taps is assumed for the channel, i.e.,

$$\mathbf{h} = \text{col}\{h_0, h_1, \ldots, h_L\} \tag{5}$$

with $L \leq P$ in order to preserve the orthogonality between tones. At the receiver, the received samples corresponding to the

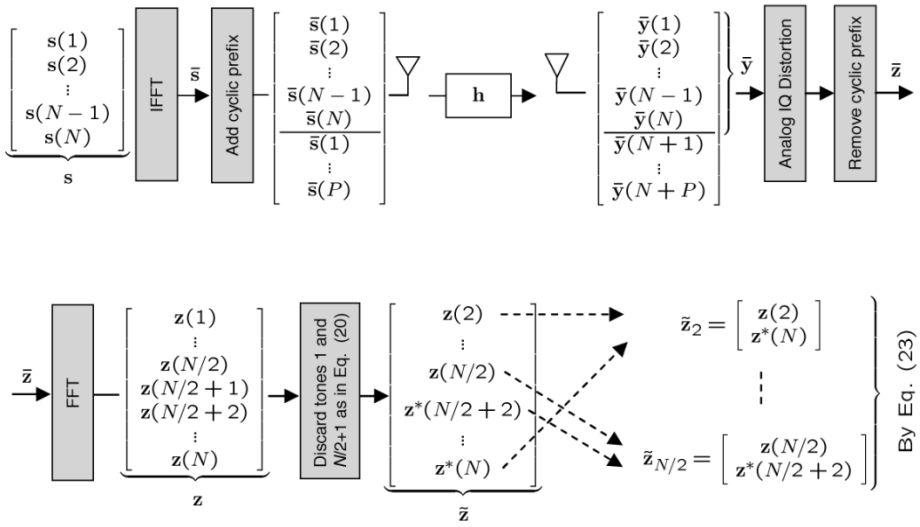

Fig. 1. OFDM receiver with IQ imbalances and the notation used in the SISO derivations.

transmitted block $\bar{\mathbf{s}}$ are collected into a vector, after discarding the received cyclic prefix samples. The received block of data before being distorted by IQ imbalances can be written as [12]:

$$\bar{\mathbf{y}} = \mathbf{H}^c \bar{\mathbf{s}} + \bar{\mathbf{v}} \tag{6}$$

where

$$\mathbf{H}^c = \begin{bmatrix} h_0 & h_1 & \cdots & h_L & & & \\ & h_0 & h_1 & \cdots & h_L & & \\ & & \ddots & & & \ddots & \\ & & & h_0 & h_1 & \cdots & h_L \\ \vdots & & & & \ddots & & \vdots \\ h_2 & \cdots h_L & & & & h_0 & h_1 \\ h_1 & \cdots & h_L & & & & h_0 \end{bmatrix} \tag{7}$$

is an $N \times N$ circulant matrix. It is known that $\mathbf{H}^c$ can be diagonalized by the N-point DFT matrix as $\mathbf{H}^c = \mathbf{F}^* \mathbf{\Lambda} \mathbf{F}$, where

$$\mathbf{\Lambda} = \text{diag}\{\lambda\} \tag{8}$$

and the vector λ is related to $\mathbf{h}$ via

$$\lambda = \sqrt{N}\mathbf{F}^* \begin{bmatrix} \mathbf{h} \\ \mathbf{0}_{(N-(L+1))\times 1} \end{bmatrix}. \tag{9}$$

Then, (6) gives

$$\bar{\mathbf{y}} = \mathbf{F}^* \mathbf{\Lambda} \mathbf{F} \bar{\mathbf{s}} + \bar{\mathbf{v}} = \mathbf{F}^* \text{diag}\{\lambda\} \mathbf{F} \bar{\mathbf{s}} + \bar{\mathbf{v}}. \tag{10}$$

The received block of data $\bar{\mathbf{y}}$ after being distorted by IQ imbalances will be transformed into [using model by (1)]

$$\bar{\mathbf{z}} = \mu \bar{\mathbf{y}} + \nu \text{conj}(\bar{\mathbf{y}}) \tag{11}$$

where the notation $\text{conj}(\bar{\mathbf{y}})$ denotes a column vector whose entries are the complex conjugates of the entries of $\bar{\mathbf{y}}$. Now remember that the N-point DFT of the complex conjugate of a sequence is related to the DFT of the original sequence through a mirrored relation (assuming $1 \le n \le N$ and $1 \le k \le N$):

$$\begin{aligned} x(n) &\xrightarrow{\text{DFT}} X(k) \\ x^*(n) &\xrightarrow{\text{DFT}} X^*(N-k+2). \end{aligned} \tag{12}$$

For notational simplicity, we denote the operation that gives the DFT of the complex conjugate of a vector by the superscript $\#$, i.e., for a vector X of size N, we write

$$X = \begin{bmatrix} X(1) \\ X(2) \\ \vdots \\ X\left(\frac{N}{2}\right) \\ X\left(\frac{N}{2}+1\right) \\ X\left(\frac{N}{2}+2\right) \\ \vdots \\ X(N) \end{bmatrix} \Longrightarrow X^{\#} = \begin{bmatrix} X^*(1) \\ X^*(N) \\ \vdots \\ X^*\left(\frac{N}{2}+2\right) \\ X^*\left(\frac{N}{2}+1\right) \\ X^*\left(\frac{N}{2}\right) \\ \vdots \\ X^*(2) \end{bmatrix} \tag{13}$$

so that if

$$X = \mathbf{F}x, \text{ then } X^{\#} = \mathbf{F}\text{conj}(x). \tag{14}$$

Now, from (6), we have

$$\text{conj}(\bar{\mathbf{y}}) = \text{conj}(\mathbf{H}^c)\text{conj}(\bar{\mathbf{s}}) + \text{conj}(\bar{\mathbf{v}}) \tag{15}$$

where $\text{conj}(\mathbf{H}^c)$ is a circulant matrix defined in terms of $\text{conj}(\mathbf{h})$, as in (7). In a manner similar to (8), (9), and (14), we have

$$\sqrt{N}\mathbf{F}^* \begin{bmatrix} \text{conj}(\mathbf{h}) \\ \mathbf{0}_{(N-(L+1))\times 1} \end{bmatrix} = \lambda^{\#} \tag{16}$$

and

$$\text{conj}(\mathbf{H}^c) = \mathbf{F}^* \text{diag}\{\lambda^{\#}\} \mathbf{F}. \tag{17}$$

Substituting the above into (15) results in

$$\begin{aligned}\text{conj}(\bar{\mathbf{y}}) &= \mathbf{F}^*\text{diag}\{\lambda^{\#}\}\mathbf{F}\text{conj}(\bar{\mathbf{s}}) + \text{conj}(\bar{\mathbf{v}}) \\ &= \mathbf{F}^*\text{diag}\{\lambda^{\#}\}\mathbf{s}^{\#} + \text{conj}(\bar{\mathbf{v}}) \end{aligned} \tag{18}$$

where $\mathbf{F}\text{conj}(\bar{\mathbf{s}})$ is replaced by $\mathbf{s}^{\#}$ using (4) and the conjugate-mirrored notation defined by (12).

Let us now consider a receiver that applies the DFT operation to the received block of data $\bar{\mathbf{z}}$, as is done in a standard OFDM receiver. Applying the DFT matrix to (11), i.e., setting $\mathbf{z} = \mathbf{F}\bar{\mathbf{z}}$, and substituting (10) and (18) into (11) lead to

$$\mathbf{z} = \mu\text{diag}\{\lambda\}\mathbf{s} + \nu\text{diag}\{\lambda^{\#}\}\mathbf{s}^{\#} + \mathbf{v} \tag{19}$$

where $\mathbf{v}$ is a transformed version of the original noise vector $\bar{\mathbf{v}}$. As seen from (19), the vector $\mathbf{z}$ is no longer related to the transmitted block $\mathbf{s}$ through a diagonal matrix, as is the case in an OFDM system with ideal I and Q branches. There is also a contribution from $\mathbf{s}^{\#}$. Discarding the samples corresponding to tones 1 and $N/2+1$, i.e., $\mathbf{z}(1)$ and $\mathbf{z}(N/2+1)$, and defining two new vectors

$$\begin{aligned}\tilde{\mathbf{z}} &= \text{col}\left\{\mathbf{z}(2), \ldots, \mathbf{z}\left(\frac{N}{2}\right), \mathbf{z}^*\left(\frac{N}{2}+2\right), \ldots, \mathbf{z}^*(N)\right\} \\ \tilde{\mathbf{s}} &= \text{col}\left\{\mathbf{s}(2), \ldots, \mathbf{s}\left(\frac{N}{2}\right), \mathbf{s}^*\left(\frac{N}{2}+2\right), \ldots, \mathbf{s}^*(N)\right\}\end{aligned} \tag{20}$$

then (19) gives (21), shown at the bottom of the page, where $\tilde{\mathbf{v}}$ is related to $\mathbf{v}$ in a manner similar to (20). Note that the matrix $\tilde{\mathbf{\Lambda}}$ in (20) is not diagonal, as is the case for $\mathbf{\Lambda}$ in (10), although it collapses to a diagonal matrix by setting ν equal to zero. Equation (21) can be reduced to 2×2 decoupled subequations, for $k = \{2, \ldots, N/2\}$, where each is written as

$$\mathbf{z}_k = \mathbf{\Gamma}_k\mathbf{s}_k + \mathbf{v}_k \tag{22}$$

where

$$\mathbf{z}_k = \begin{bmatrix} (k) \\ \mathbf{z}^*(N-k+2)\end{bmatrix}, \quad \mathbf{s}_k = \begin{bmatrix} (k) \\ \mathbf{s}^*(N-k+2)\end{bmatrix} \tag{23}$$

$$\mathbf{\Gamma}_k = \begin{bmatrix} \mu\lambda(k) & \nu\lambda^*(N-k+2) \\ \nu^*\lambda(k) & \mu^*\lambda^*(N-k+2)\end{bmatrix}. \tag{24}$$

The objective is to recover $\mathbf{s}_k$ from $\mathbf{z}_k$ in (22) for $k = \{2, \ldots, N/2\}$ or, equivalently, $\tilde{\mathbf{s}}$ from $\tilde{\mathbf{z}}$ in (21). Several algorithms, adaptive and otherwise, for estimating channel/distortion parameters and recovering the $\mathbf{s}_k$ were proposed in [3]. The situation is more challenging in the MIMO case. The objective of this paper is to describe and address the difficulties that arise in the MIMO case. The paper will also show how to exploit the structure of space-time block codes in order to simplify the resulting MIMO OFDM receivers in the presence of IQ imbalances.

III. MIMO OFDM Systems

First, we introduce the notation for the MIMO case:

- n_T: number of transmit antennas
- n_R: number of receive antennas
- $L_{m,l}+1$: number of channel taps from transmit antenna l to receive antenna m
- μ_m and ν_m: parameter modeling IQ imbalance for the receive antenna m, as defined by (2)
- $\mathbf{h}_{m,l}$: channel taps from transmit antenna l to receive antenna m, as defined by (5); see Fig. 2
- $\mathbf{s}_l$ and $\bar{\mathbf{s}}_l$: block of data and its inverse Fourier transform transmitted by antenna l, as defined by (4)
- $\bar{\mathbf{y}}_m$: received block of data by antenna m before distortion by IQ imbalances, as defined by (6)
- $\bar{\mathbf{z}}_m$: received block of data by antenna m after distortion by IQ imbalances, as defined by (11)(the cyclic prefix samples are eliminated at this stage from the received block of data)
- $\mathbf{H}^c_{m,l}$: square circulant matrix defined as in (7) corresponding to the channel from antenna l to antenna m.

The superscript (M) is added to the vectors in this section (MIMO case) to differentiate them from the corresponding ones in the SISO case. Using the structure shown in Fig. 2, data blocks received on different antennas $\bar{\mathbf{z}}_m$ for $m = \{1, \ldots, n_R\}$ are collected into a column vector of size $n_R N$. As shown in [13], the received blocks of data on different receive antennas before distortion by IQ imbalances are given by [using a similar structure as in (6) and (7)]

$$\underbrace{\begin{bmatrix}\bar{\mathbf{y}}_{n_R} \\ \vdots \\ \bar{\mathbf{y}}_1\end{bmatrix}}_{\bar{\mathbf{y}}^{(M)}} = \underbrace{\begin{bmatrix}\mathbf{H}^c_{n_R,n_T} & \cdots & \mathbf{H}^c_{n_R,1} \\ \vdots & \ddots & \vdots \\ \mathbf{H}^c_{1,n_T} & \cdots & \mathbf{H}^c_{1,1}\end{bmatrix}}_{\mathbf{H}^{(M)}} \underbrace{\begin{bmatrix}\bar{\mathbf{s}}_{n_T} \\ \vdots \\ \bar{\mathbf{s}}_1\end{bmatrix}}_{\bar{\mathbf{s}}^{(M)}} + \bar{\mathbf{v}}^{(M)} \tag{25}$$

where $\bar{\mathbf{v}}^{(M)}$ contains the additive noise on all receive antennas, and $\mathbf{H}^c_{m,l}$, $m = \{1, \ldots, n_R\}$, and $l = \{1, \ldots, n_T\}$ are diago-

$$\tilde{\mathbf{z}} = \underbrace{\begin{bmatrix} \mu\lambda(2) & & & & & & \nu\lambda^*(N) \\ & \ddots & & & & \iddots & \\ & & \mu\lambda\left(\frac{N}{2}\right) & \nu\lambda^*\left(\frac{N}{2}+2\right) & & & \\ & & \nu^*\lambda\left(\frac{N}{2}\right) & \mu^*\lambda^*\left(\frac{N}{2}+2\right) & & & \\ & \iddots & & & & \ddots & \\ \nu^*\lambda(2) & & & & & & \mu^*\lambda^*(N)\end{bmatrix}}_{\tilde{\mathbf{\Lambda}}} \tilde{\mathbf{s}} + \tilde{\mathbf{v}} \tag{21}$$

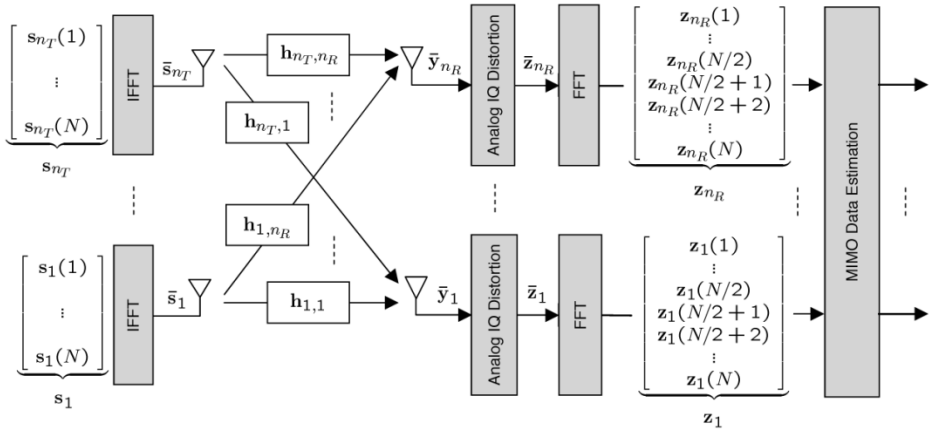

Fig. 2. OFDM-based MIMO system with IQ imbalances. The data estimation block is shown in Fig. 3(b) based on the notation developed in Section III.

nalized by the DFT operation as $\mathbf{H}^c_{m,l} = \mathbf{F}^*\mathbf{\Lambda}_{m,l}\mathbf{F}$. As in (11), the received block of data after distortion by IQ imbalances becomes

$$\underbrace{\begin{bmatrix} \bar{\mathbf{z}}_{n_R} \\ \vdots \\ \bar{\mathbf{z}}_1 \end{bmatrix}}_{\bar{\mathbf{z}}^{(M)}} = \begin{bmatrix} \mu_{n_R}\bar{\mathbf{y}}_{n_R} \\ \vdots \\ \mu_1\bar{\mathbf{y}}_1 \end{bmatrix} + \begin{bmatrix} \nu_{n_R}\text{conj}(\bar{\mathbf{y}}_{n_R}) \\ \vdots \\ \nu_1\text{conj}(\bar{\mathbf{y}}_1) \end{bmatrix}. \tag{26}$$

Using the formulation and notation that led to (19) and by defining

$$\mathbf{z}_m = \mathbf{F}\bar{\mathbf{z}}_m \tag{27}$$

for $m = \{1, \ldots, n_R\}$, (26) leads to (28), shown at the bottom of the page. The definitions in (20) and the argument that led from (19) to (21) can be applied to (28). Let

$$\tilde{\mathbf{z}}_m = \text{col}\left\{\mathbf{z}_m(2), \ldots, \mathbf{z}_m\left(\frac{N}{2}\right) \mathbf{z}^*_m\left(\frac{N}{2}+2\right), \ldots, \mathbf{z}^*_m(N)\right\} \tag{29}$$

for $m = \{1, \ldots, n_R\}$, and

$$\tilde{\mathbf{s}}_l = \text{col}\left\{\mathbf{s}_l(2), \ldots, \mathbf{s}_l\left(\frac{N}{2}\right), \mathbf{s}^*_l\left(\frac{N}{2}+2\right), \ldots, \mathbf{s}^*_l(N)\right\} \tag{30}$$

for $l = \{1, \ldots, n_T\}$. Using these definitions, (28) becomes

$$\begin{bmatrix} \tilde{\mathbf{z}}_{n_R} \\ \vdots \\ \tilde{\mathbf{z}}_1 \end{bmatrix} = \underbrace{\begin{bmatrix} \tilde{\Lambda}_{n_R,n_T} & \cdots & \tilde{\Lambda}_{n_R,1} \\ \vdots & \ddots & \vdots \\ \tilde{\Lambda}_{1,n_T} & \cdots & \tilde{\Lambda}_{1,1} \end{bmatrix}}_{\tilde{\Lambda}^{(M)}} \begin{bmatrix} \tilde{\mathbf{s}}_{n_T} \\ \vdots \\ \tilde{\mathbf{s}}_1 \end{bmatrix} + \begin{bmatrix} \tilde{\mathbf{v}}_{n_R} \\ \vdots \\ \tilde{\mathbf{v}}_1 \end{bmatrix} \tag{31}$$

where each $\tilde{\Lambda}_{m,l}$ is defined as in (21) for the channel from transmit antenna l to receive antenna m:

$$\tilde{\Lambda}_{m,l} = \begin{bmatrix} \mu_m\lambda_{m,l}(2) & & \nu_m\lambda^*_{m,l}(N) \\ & \ddots & \\ & \mu_m\lambda_{m,l}\left(\frac{N}{2}\right) \quad \nu_m\lambda^*_{m,l}\left(\frac{N}{2}+2\right) & \\ & \nu^*_m\lambda_{m,l}\left(\frac{N}{2}\right) \quad \mu^*_m\lambda^*_{m,l}\left(\frac{N}{2}+2\right) & \\ & \ddots & \\ \nu^*_m\lambda_{m,l}(2) & & \mu^*_m\lambda^*_{m,l}(N) \end{bmatrix}. \tag{32}$$

The main difference between the above system (with IQ imbalances) and a MIMO OFDM system with ideal I and Q branches lies in the value of the subblocks $\tilde{\Lambda}_{m,l}$. In a MIMO OFDM system with ideal I and Q branches, these subblock matrices are diagonal [12], [13]. It can be easily seen that the system defined by (31) and (32) collapses to the ideal MIMO OFDM system by replacing ν_m, $m = \{1, \ldots, n_R\}$, with zero, as is expected.

Rather than continue with the system defined by (31), this system can be reduced to smaller dimension subsystems.

$$\begin{bmatrix} \mathbf{z}_{n_R} \\ \vdots \\ \mathbf{z}_1 \end{bmatrix} = \begin{bmatrix} \mu_{n_R}\text{diag}\{\lambda_{n_R,n_T}\} & \cdots & \mu_{n_R}\text{diag}\{\lambda_{n_R,1}\} \\ \vdots & \ddots & \vdots \\ \mu_1\text{diag}\{\lambda_{1,n_T}\} & \cdots & \mu_1\text{diag}\{\lambda_{1,1}\} \end{bmatrix} \begin{bmatrix} \mathbf{s}_{n_T} \\ \vdots \\ \mathbf{s}_1 \end{bmatrix} + \begin{bmatrix} \nu_{n_R}\text{diag}\left\{\lambda^{\#}_{n_R,n_T}\right\} & \cdots & \nu_{n_R}\text{diag}\left\{\lambda^{\#}_{n_R,1}\right\} \\ \vdots & \ddots & \vdots \\ \nu_1\text{diag}\left\{\lambda^{\#}_{1,n_T}\right\} & \cdots & \nu_1\text{diag}\left\{\lambda^{\#}_{1,1}\right\} \end{bmatrix} \begin{bmatrix} \mathbf{s}^{\#}_{n_T} \\ \vdots \\ \mathbf{s}^{\#}_1 \end{bmatrix} + \mathbf{v}^{(M)}. \tag{28}$$

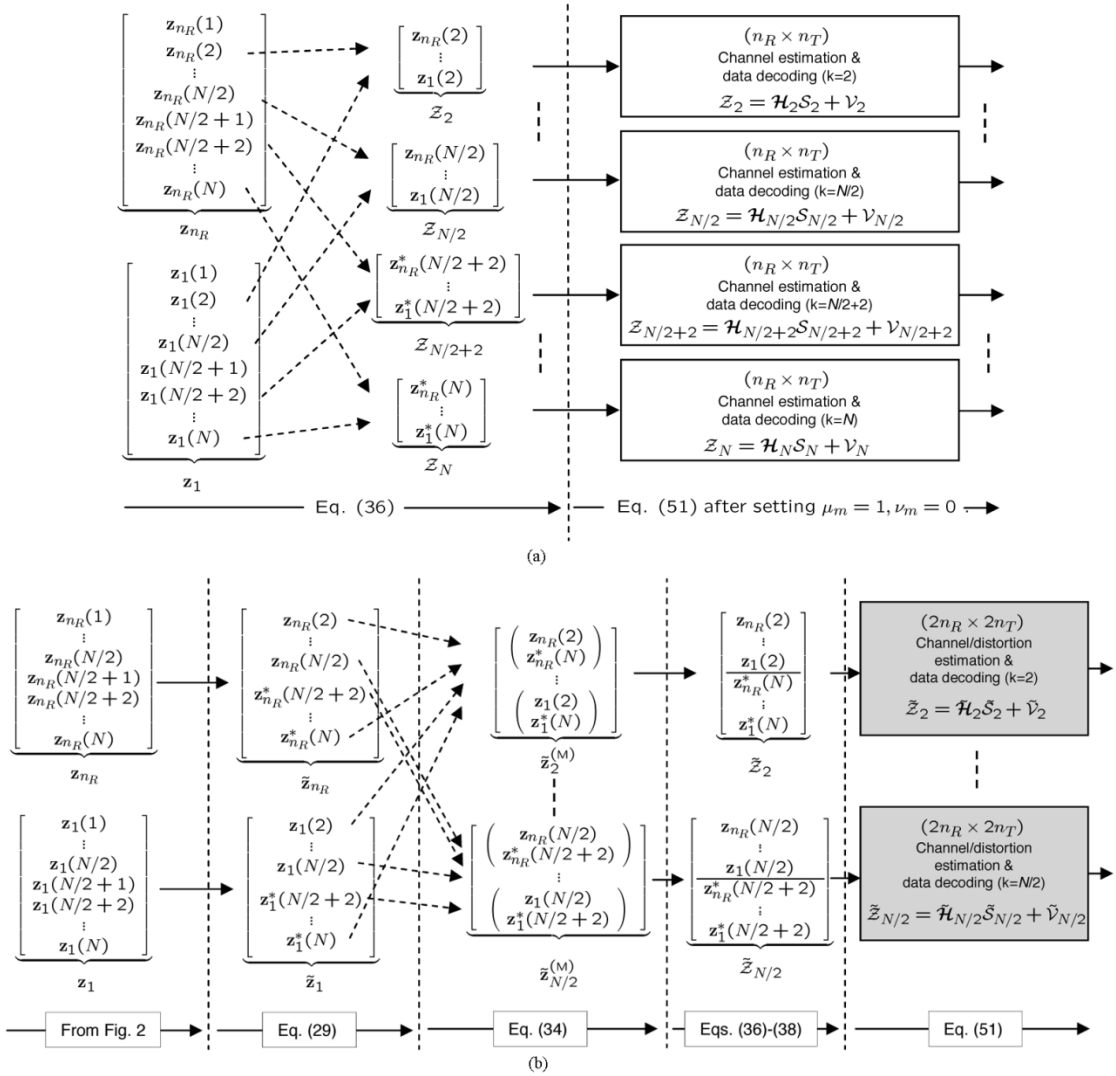

Fig. 3. Derived MIMO OFDM receiver in Section III, considering IQ imbalances, is compared to a standard MIMO OFDM receiver that assumes ideal IQ branches. The notation used in these figures is consistent with the notation developed in Section III. The proposed receiver structure in (b) collapses to the standard structure in (a) by substituting $\mu_m = 1$ and $\nu_m = 0, m = \{1, \ldots, n_R\}$ in (51). (a) Standard MIMO OFDM receiver assuming *ideal* IQ branches. (b) Proposed MIMO OFDM receiver in the presence of IQ *imbalances*.

The subblocks resulting from regrouping terms are an extension of the structure defined by (23) and (24), such that for $k = \{2, \ldots, N/2\}$

$$\tilde{\mathbf{z}}_k^{(M)} = \tilde{\mathbf{\Gamma}}_k^{(M)} \tilde{\mathbf{s}}_k^{(M)} + \tilde{\mathbf{v}}_k^{(M)} \tag{33}$$

where the pertinent quantities are defined by (34) and (35), shown at the bottom of the next page. A MIMO OFDM receiver using the above system of equations is shown in Fig. 3(b). For comparison purposes, a standard receiver structure assuming ideal IQ branches is depicted in Fig. 3(a). Note that the $(2n_R \times 2n_T)$ set of equations given by (33) reduces to two decoupled $(n_R \times n_T)$ sets of equations by substituting $\mu_m = 1$ and $\nu_m = 1, m = \{1, \ldots, n_R\}$, as is expected for the case of a MIMO OFDM receiver assuming ideal IQ branches.

From (33), it can be seen that a receiver for the MIMO OFDM system with IQ imbalances would have to solve $(N/2-1)$ subsystems of dimension $2n_R \times 2n_T$ each. In comparison, a receiver for MIMO OFDM with ideal I and Q branches needs to solve $(N-2)$ subsystems of dimension $n_R \times n_T$ each. The presence of IQ imbalances basically couples every tone with its mirrored tone, i.e., k and $(N-k+2)$.

Although the system of (33) completely specifies the input–output relation in the MIMO case, we will rearrange the input–output vectors into a format that will be useful for studying space-time block-coded systems. With the same notation used in (34) and (35), we introduce the following vectors for $k = \{2, \ldots, N/2\}$:

$$\mathcal{Z}_k = \begin{bmatrix} \mathbf{z}_{n_R}(k) \\ \vdots \\ \mathbf{z}_1(k) \end{bmatrix}, \quad \mathcal{Z}_{N-k+2} = \begin{bmatrix} \mathbf{z}_{n_R}^*(N-k+2) \\ \vdots \\ \mathbf{z}_1^*(N-k+2) \end{bmatrix} \tag{36}$$

and

$$\mathcal{S}_k = \begin{bmatrix} \mathbf{s}_{n_T}(k) \\ \vdots \\ \mathbf{s}_1(k) \end{bmatrix}, \quad \mathcal{S}_{N-k+2} = \begin{bmatrix} \mathbf{s}_{n_T}^*(N-k+2) \\ \vdots \\ \mathbf{s}_1^*(N-k+2) \end{bmatrix} \tag{37}$$

and use (33) to conclude that

$$\underbrace{\left[\begin{array}{c}\mathcal{Z}_k\\ \hline \mathcal{Z}_{N-k+2}\end{array}\right]}_{\tilde{\mathcal{Z}}_k} = \left[\begin{array}{c|c}\boldsymbol{\Lambda}_k^{(M)} & \boldsymbol{\Phi}_{N-k+2}^{(M)}\\ \hline \boldsymbol{\Phi}_k^{(M)} & \boldsymbol{\Lambda}_{N-k+2}^{(M)}\end{array}\right] \underbrace{\left[\begin{array}{c}\mathcal{S}_k\\ \hline \mathcal{S}_{N-k+2}\end{array}\right]}_{\tilde{\mathcal{S}}_k} + \underbrace{\left[\begin{array}{c}\mathcal{V}_k\\ \hline \mathcal{V}_{N-k+2}\end{array}\right]}_{\tilde{\mathcal{V}}_k} \quad (38)$$

where we have (39)–(42), shown at the bottom of the page. The above matrices are related to the channel tap matrices as follows. Collect the channel taps from the n_T transmit antennas to the n_R receive antennas corresponding to the kth tone into

$$\boldsymbol{\mathcal{H}}_k = \begin{bmatrix} \lambda_{n_R,n_T}(k) & \dots & \lambda_{n_R,1}(k) \\ \vdots & \ddots & \vdots \\ \lambda_{1,n_T}(k) & \dots & \lambda_{1,1}(k) \end{bmatrix} \quad (43)$$

and similarly for the $(N-k+2)$th tone

$$\boldsymbol{\mathcal{H}}_{N-k+2} = \begin{bmatrix} \lambda_{n_R,n_T}^*(N-k+2) & \dots & \lambda_{n_R,1}^*(N-k+2) \\ \vdots & \ddots & \vdots \\ \lambda_{1,n_T}^*(N-k+2) & \dots & \lambda_{1,1}^*(N-k+2) \end{bmatrix}. \quad (44)$$

By defining two diagonal matrices representing the distortion parameters on different receive antennas as

$$\boldsymbol{\Pi}_\mu = \begin{bmatrix} \mu_{n_R} & \dots & 0 \\ \vdots & \ddots & \vdots \\ 0 & \dots & \mu_1 \end{bmatrix} \quad (45)$$

$$\boldsymbol{\Pi}_\nu = \begin{bmatrix} \nu_{n_R} & \dots & 0 \\ \vdots & \ddots & \vdots \\ 0 & \dots & \nu_1 \end{bmatrix} \quad (46)$$

the submatrices $\boldsymbol{\Lambda}_k^{(M)}$, $\boldsymbol{\Phi}_{N-k+2}^{(M)}$, $\boldsymbol{\Phi}_k^{(M)}$, and $\boldsymbol{\Lambda}_{N-k+2}^{(M)}$ can be

$$\tilde{\mathbf{z}}_k^{(M)} = \underbrace{\left[\begin{array}{c}\begin{pmatrix}\mathbf{z}_{n_R}(k)\\ \mathbf{z}_{n_R}^*(N-k+2)\end{pmatrix}\\ \hline \vdots \\ \hline \begin{pmatrix}\mathbf{z}_1(k)\\ \mathbf{z}_1^*(N-k+2)\end{pmatrix}\end{array}\right]}_{2n_R\times 1}, \quad \tilde{\mathbf{s}}_k^{(M)} = \underbrace{\left[\begin{array}{c}\begin{pmatrix}\mathbf{s}_{n_T}(k)\\ \mathbf{s}_{n_T}^*(N-k+2)\end{pmatrix}\\ \hline \vdots \\ \hline \begin{pmatrix}\mathbf{s}_1(k)\\ \mathbf{s}_1^*(N-k+2)\end{pmatrix}\end{array}\right]}_{2n_T\times 1} \quad (34)$$

$$\tilde{\boldsymbol{\Gamma}}_k^{(M)} = \underbrace{\begin{bmatrix} \begin{pmatrix}\mu_{n_R}\lambda_{n_R,n_T}(k) & \nu_{n_R}\lambda_{n_R,n_T}^*(N-k+2)\\ \nu_{n_R}^*\lambda_{n_R,n_T}(k) & \mu_{n_R}^*\lambda_{n_R,n_T}^*(N-k+2)\end{pmatrix} & \dots & \begin{pmatrix}\mu_{n_R}\lambda_{n_R,1}(k) & \nu_{n_R}\lambda_{n_R,1}^*(N-k+2)\\ \nu_{n_R}^*\lambda_{n_R,1}(k) & \mu_{n_R}^*\lambda_{n_R,1}^*(N-k+2)\end{pmatrix} \\ \vdots & & \vdots \\ \begin{pmatrix}\mu_1\lambda_{1,n_T}(k) & \nu_1\lambda_{1,n_T}^*(N-k+2)\\ \nu_1^*\lambda_{1,n_T}(k) & \mu_1^*\lambda_{1,n_T}^*(N-k+2)\end{pmatrix} & \dots & \begin{pmatrix}\mu_1\lambda_{1,1}(k) & \nu_1\lambda_{1,1}^*(N-k+2)\\ \nu_1^*\lambda_{1,1}(k) & \mu_1^*\lambda_{1,1}^*(N-k+2)\end{pmatrix} \end{bmatrix}}_{2n_R\times 2n_T}. \quad (35)$$

$$\boldsymbol{\Lambda}_k^{(M)} = \begin{bmatrix} \mu_{n_R}\lambda_{n_R,n_T}(k) & \dots & \mu_{n_R}\lambda_{n_R,1}(k) \\ \vdots & \ddots & \vdots \\ \mu_1\lambda_{1,n_T}(k) & \dots & \mu_1\lambda_{1,1}(k) \end{bmatrix} \quad (39)$$

$$\boldsymbol{\Phi}_k^{(M)} = \begin{bmatrix} \nu_{n_R}^*\lambda_{n_R,n_T}(k) & \dots & \nu_{n_R}^*\lambda_{n_R,1}(k) \\ \vdots & \ddots & \vdots \\ \nu_1^*\lambda_{1,n_T}(k) & \dots & \nu_1^*\lambda_{1,1}(k) \end{bmatrix} \quad (40)$$

$$\boldsymbol{\Phi}_{N-k+2}^{(M)} = \begin{bmatrix} \nu_{n_R}\lambda_{n_R,n_T}^*(N-k+2) & \dots & \nu_{n_R}\lambda_{n_R,1}^*(N-k+2) \\ \vdots & \ddots & \vdots \\ \nu_1\lambda_{1,n_T}^*(N-k+2) & \dots & \nu_1\lambda_{1,1}^*(N-k+2) \end{bmatrix} \quad (41)$$

$$\boldsymbol{\Lambda}_{N-k+2}^{(M)} = \begin{bmatrix} \mu_{n_R}^*\lambda_{n_R,n_T}^*(N-k+2) & \dots & \mu_{n_R}^*\lambda_{n_R,1}^*(N-k+2) \\ \vdots & \ddots & \vdots \\ \mu_1^*\lambda_{1,n_T}^*(N-k+2) & \dots & \mu_1^*\lambda_{1,1}^*(N-k+2) \end{bmatrix}. \quad (42)$$

then written as

$$\mathbf{\Lambda}_k^{(M)} = \mathbf{\Pi}_\mu \mathcal{H}_k \tag{47}$$

$$\mathbf{\Phi}_k^{(M)} = \mathbf{\Pi}_\nu^* \mathcal{H}_k \tag{48}$$

$$\mathbf{\Phi}_{N-k+2}^{(M)} = \mathbf{\Pi}_\nu \mathcal{H}_{N-k+2} \tag{49}$$

$$\mathbf{\Lambda}_{N-k+2}^{(M)} = \mathbf{\Pi}_\mu^* \mathcal{H}_{N-k+2}. \tag{50}$$

Using the above relations, (38) becomes

$$\underbrace{\left[\begin{array}{c} \mathcal{Z}_k \\ \hline \mathcal{Z}_{N-k+2} \end{array}\right]}_{2n_R \times 1} = \underbrace{\left[\begin{array}{c|c} \mathbf{\Pi}_\mu \mathcal{H}_k & \mathbf{\Pi}_\nu \mathcal{H}_{N-k+2} \\ \hline \mathbf{\Pi}_\nu^* \mathcal{H}_k & \mathbf{\Pi}_\mu^* \mathcal{H}_{N-k+2} \end{array}\right]}_{2n_R \times 2n_T} \underbrace{\left[\begin{array}{c} \mathcal{S}_k \\ \hline \mathcal{S}_{N-k+2} \end{array}\right]}_{2n_T \times 1} + \left[\begin{array}{c} \mathcal{V}_k \\ \hline \mathcal{V}_{N-k+2} \end{array}\right]. \tag{51}$$

Comparing the above equation with (23) and (24), we see that this system of equations is an extension of the framework derived for SISO OFDM receivers.

The system of equations (51) can be used to estimate the transmitted data $\mathcal{S}_k$ and $\mathcal{S}_{N-k+2}$ from the received data $\mathcal{Z}_k$ and $\mathcal{Z}_{N-k+2}$, given the assumption that no space-time coding is incorporated into the transmitted data $\mathcal{S}_k$ and $\mathcal{S}_{N-k+2}$.[2] For instance, maximum-likelihood (ML), least-squares (LS), or minimum mean-square-error (MMSE) algorithms can be developed at the receiver based on (51). However, in the presence of space-time coded transmission, the system of equations by (51) can be reworked to exploit the structure of the space-time codes. In Sections IV–VI, the structure of space-time block codes is exploited to derive efficient receiver algorithms to compensate for IQ imbalances.

IV. MIMO Receiver With Space-Time Block Coding

In a MIMO OFDM system, space-time coding is typically applied independently on each tone $k = \{1, \ldots, N\}$. In other words, independent blocks of space-time coded data are transmitted through each tone. To incorporate space-time coding into (34) and (35), a superscript is added to represent the time instant. To be more specific, we have the following.

- $\mathbf{s}_{j,i}(k)$ will represent the transmitted data on tone k and transmit antenna j at time instant i.
- $\mathbf{z}_{j,i}(k)$ will represent the corresponding received data on tone k and receive antenna j at time instant i.
- $\mathcal{S}_{k,i}$ contains the transmitted data on tone k from all antennas at time instant i, i.e., $\mathcal{S}_{k,i} = \text{col}\{\mathbf{s}_{n_T,i}(k), \ldots, \mathbf{s}_{1,i}(k)\}$.

Now, assume that the transmitter uses a space-time block code of size $(n_T \times p)$, where p is the depth of the block code in time. In this case, a block of data is transmitted, and each block contains a collection of vectors $\mathcal{S}_{k,1}$ through $\mathcal{S}_{k,p}$, which is defined by (37), say

$$\boldsymbol{\mathcal{S}}_k^{(B)} \triangleq [\,\mathcal{S}_{k,p} \;|\; \ldots \;|\; \mathcal{S}_{k,1}\,] = \begin{bmatrix} \mathbf{s}_{n_T,p}(k) & \ldots & \mathbf{s}_{n_T,1}(k) \\ \vdots & & \vdots \\ \mathbf{s}_{1,p}(k) & \ldots & \mathbf{s}_{1,1}(k) \end{bmatrix} \tag{52}$$

[2]For example, the BLAST structures introduced in [14] and [15] should use the $(2n_R \times 2n_T)$ system of equations given by (51) instead of the $(n_R \times n_T)$ system of equations used in standard MIMO systems.

and a similar structure holds for $\boldsymbol{\mathcal{S}}_{N-k+2}^{(B)}$. Similarly, the corresponding received block of data is

$$\boldsymbol{\mathcal{Z}}_k^{(B)} \triangleq [\,\mathcal{Z}_{k,p} \;|\; \ldots \;|\; \mathcal{Z}_{k,1}\,] = \begin{bmatrix} \mathbf{z}_{n_R,p}(k) & \ldots & \mathbf{z}_{n_R,1}(k) \\ \vdots & & \vdots \\ \mathbf{z}_{1,p}(k) & \ldots & \mathbf{s}_{1,1}(k) \end{bmatrix} \tag{53}$$

and a similar structure holds for $\boldsymbol{\mathcal{Z}}_{N-k+2}^{(B)}$.

Using the above notation in (51), the transmitted and received blocks of data are now related through

$$\underbrace{\left[\begin{array}{c} \boldsymbol{\mathcal{Z}}_k^{(B)} \\ \hline \boldsymbol{\mathcal{Z}}_{N-k+2}^{(B)} \end{array}\right]}_{\tilde{\boldsymbol{\mathcal{Z}}}_k^{(B)}:2n_R \times p} = \underbrace{\left[\begin{array}{c|c} \mathbf{\Pi}_\mu \mathcal{H}_k & \mathbf{\Pi}_\nu \mathcal{H}_{N-k+2} \\ \hline \mathbf{\Pi}_\nu^* \mathcal{H}_k & \mathbf{\Pi}_\mu^* \mathcal{H}_{N-k+2} \end{array}\right]}_{\tilde{\mathcal{H}}_k:2n_R \times 2n_T} \underbrace{\left[\begin{array}{c} \boldsymbol{\mathcal{S}}_k^{(B)} \\ \hline \boldsymbol{\mathcal{S}}_{N-k+2}^{(B)} \end{array}\right]}_{\tilde{\boldsymbol{\mathcal{S}}}_k^{(B)}:2n_T \times p} + \underbrace{\left[\begin{array}{c} \boldsymbol{\mathcal{V}}_k^{(B)} \\ \hline \boldsymbol{\mathcal{V}}_{N-k+2}^{(B)} \end{array}\right]}_{\tilde{\boldsymbol{\mathcal{V}}}_k^{(B)}:2n_R \times p}. \tag{54}$$

This system of equations should be used to estimate $\tilde{\boldsymbol{\mathcal{S}}}_k^{(B)}$ from $\tilde{\boldsymbol{\mathcal{Z}}}_k^{(B)}$.

Based on the desired decoding algorithm, different receiver structures could be considered at the receiver. For instance, either the maximum-likelihood receiver or the least-squares receiver could be implemented. The maximum likelihood receiver estimates $\tilde{\boldsymbol{\mathcal{S}}}_k^{(B)}$, $k = \{2, \ldots, N/2\}$, according to

$$\hat{\tilde{\boldsymbol{\mathcal{S}}}}_k^{(B)} = \arg \min_{\tilde{\boldsymbol{\mathcal{S}}}_k^{(B)} \in \boldsymbol{\mathcal{S}}^{(B)}} \left\| \tilde{\boldsymbol{\mathcal{Z}}}_k^{(B)} - \tilde{\mathcal{H}}_k \tilde{\boldsymbol{\mathcal{S}}}_k^{(B)} \right\|^2$$

where $\boldsymbol{\mathcal{S}}^{(B)}$ represents the codebook for the transmitted blocks of data.

V. Alamouti Scheme With IQ Imbalances

The space-time structure of the transmitted blocks of data can be exploited in order to derive efficient receiver structures. We illustrate this fact by considering first the case of an Alamouti scheme with a 2-transmit and 1-receive antenna. Thus, let $n_T = 2$ and $n_R = 1$. In the Alamouti scheme, symbols $\{s_2, s_1\}$ are transmitted at the first time instant, followed by $\{s_1^*, -s_2^*\}$ at the second time instant [16]. An OFDM-based Alamouti scheme is depicted in Fig. 4. In this case, the space-time block code given by (52) reduces to

$$\boldsymbol{\mathcal{S}}_k^{(B)} = \underbrace{\begin{bmatrix} \mathbf{s}_{1,1}^*(k) & \mathbf{s}_{2,1}(k) \\ -\mathbf{s}_{2,1}^*(k) & \mathbf{s}_{1,1}(k) \end{bmatrix}}_{\mathcal{S}_{k,2} \quad \mathcal{S}_{k,1}} \tag{55}$$

and, similarly

$$\boldsymbol{\mathcal{S}}_{N-k+2}^{(B)} = \begin{bmatrix} \mathbf{s}_{1,1}(N-k+2) & \mathbf{s}_{2,1}^*(N-k+2) \\ -\mathbf{s}_{2,1}(N-k+2) & \mathbf{s}_{1,1}^*(N-k+2) \end{bmatrix}. \tag{56}$$

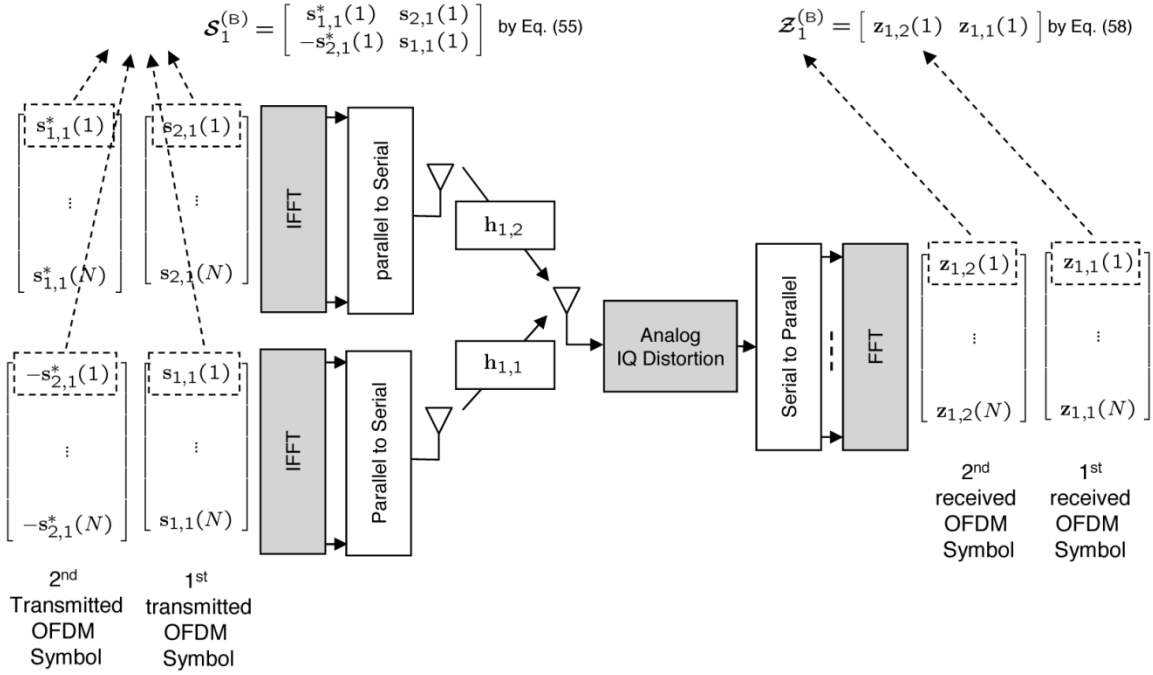

Fig. 4. Alamouti scheme applied to an OFDM system.

The transmitted block of data $\tilde{\mathcal{S}}_k^{(B)}$ defined in (54) is therefore given by

$$\tilde{\mathcal{S}}_k^{(B)} = \left[\frac{\mathcal{S}_k^{(B)}}{\mathcal{S}_{N-k+2}^{(B)}}\right] = \left[\begin{array}{cc} \mathbf{s}_{1,1}^*(k) & \mathbf{s}_{2,1}(k) \\ -\mathbf{s}_{2,1}^*(k) & \mathbf{s}_{1,1}(k) \\ \hline \mathbf{s}_{1,1}(N-k+2) & \mathbf{s}_{2,1}^*(N-k+2) \\ -\mathbf{s}_{2,1}(N-k+2) & \mathbf{s}_{1,1}^*(N-k+2) \end{array}\right]. \quad (57)$$

Similarly, the corresponding received block of data $\tilde{\mathcal{Z}}_k^{(B)}$ defined in (54) becomes

$$\tilde{\mathcal{Z}}_k^{(B)} = \left[\frac{\mathcal{Z}_k^{(B)}}{\mathcal{Z}_{N-k+2}^{(B)}}\right] = \left[\begin{array}{cc} \mathbf{z}_{1,2}(k) & \mathbf{z}_{1,1}(k) \\ \hline \mathbf{z}_{1,2}^*(N-k+2) & \mathbf{z}_{1,1}^*(N-k+2) \end{array}\right]. \quad (58)$$

These two blocks are related through the matrix $\tilde{\mathcal{H}}_k$ defined in (54)

$$\underbrace{\tilde{\mathcal{Z}}_k^{(B)}}_{2\times 2} = \underbrace{\tilde{\mathcal{H}}_k}_{2\times 4}\underbrace{\tilde{\mathcal{S}}_k^{(B)}}_{4\times 2} + \underbrace{\tilde{\mathcal{V}}_k^{(B)}}_{2\times 2} \quad (59)$$

where for the case of a 2-transmit 1-receive antenna, the matrix $\tilde{\mathcal{H}}_k$ is given by (60), shown at the bottom of the page, by using (43)–(46).

For a moment, let us consider an ideal receiver. In this case, the relation between $\tilde{\mathcal{S}}_k^{(B)}$ and $\tilde{\mathcal{Z}}_k^{(B)}$ reduces to two decoupled systems of equations for tones k and $(N-k+2)$. For instance, for the data transmitted on tone k, the system of equations becomes

$$\underbrace{\mathcal{Z}_k^{(B)}}_{1\times 2} = \underbrace{\mathcal{H}_k}_{1\times 2}\underbrace{\mathcal{S}_k^{(B)}}_{2\times 2} + \underbrace{\mathcal{V}_k^{(B)}}_{1\times 2} \quad (61)$$

with

$$\mathcal{H}_k = [\,\lambda_{1,2}(k) \quad \lambda_{1,1}(k)\,]. \quad (62)$$

Equations (61) and (62) can be reorganized as follows. Let

$$\mathcal{Z}_k^{(\mathrm{Al})} = \begin{bmatrix} \mathbf{z}_{1,1}(k) \\ \mathbf{z}_{1,2}^*(k) \end{bmatrix} \qquad \mathcal{S}_k^{(\mathrm{Al})} = \begin{bmatrix} \mathbf{s}_{2,1}(k) \\ \mathbf{s}_{1,1}(k) \end{bmatrix}. \quad (63)$$

Then, as is well-known, (61) becomes

$$\underbrace{\mathcal{Z}_k^{(\mathrm{Al})}}_{2\times 1} = \underbrace{\mathcal{G}_k}_{2\times 2}\underbrace{\mathcal{S}_k^{(\mathrm{Al})}}_{2\times 1} + \underbrace{\mathcal{V}_k^{(\mathrm{Al})}}_{2\times 1} \quad (64)$$

where

$$\mathcal{G}_k = \begin{bmatrix} \lambda_{1,2}(k) & \lambda_{1,1}(k) \\ -\lambda_{1,1}^*(k) & \lambda_{1,2}^*(k) \end{bmatrix}. \quad (65)$$

$$\tilde{\mathcal{H}}_k = \left[\begin{array}{cc|cc} \mu_1\lambda_{1,2}(k) & \mu_1\lambda_{1,1}(k) & \nu_1\lambda_{1,2}^*(N-k+2) & \nu_1\lambda_{1,1}^*(N-k+2) \\ \nu_1^*\lambda_{1,2}(k) & \nu_1^*\lambda_{1,1}(k) & \mu_1^*\lambda_{1,2}^*(N-k+2) & \mu_1^*\lambda_{1,1}^*(N-k+2) \end{array}\right]. \quad (60)$$

Recovering $\mathcal{S}_k^{(\mathrm{Al})}$ from $\mathcal{Z}_k^{(\mathrm{Al})}$ and using (64) and (65) is a decoupled estimation problem, and it achieves full diversity due to the following orthogonality property:

$$\boldsymbol{\mathcal{G}}_k^* \boldsymbol{\mathcal{G}}_k = (|\lambda_{1,1}(k)|^2 + |\lambda_{1,2}(k)|^2)\mathbf{I}_{2\times 2} \tag{66}$$

where $\mathbf{I}_{2\times 2}$ is the identity matrix. The procedure that led from (61) to (64) for an ideal receiver can be applied to (59) for a receiver with IQ distortion.

Indeed, one can verify that repeating the above procedure for $\boldsymbol{\mathcal{Z}}_k^{(B)}$ and $\boldsymbol{\mathcal{Z}}_{N-k+2}^{(B)}$ in (58) [and, correspondingly, $\boldsymbol{\mathcal{S}}_k^{(B)}$ and $\boldsymbol{\mathcal{S}}_{N-k+2}^{(B)}$ in (57)] will result in the following structure. Let

$$\tilde{\mathcal{S}}_k^{(\mathrm{Al})} = \begin{bmatrix} \mathcal{S}_k^{(\mathrm{Al})} \\ \hline \mathcal{S}_{N-k+2}^{(\mathrm{Al})} \end{bmatrix} = \begin{bmatrix} \mathbf{s}_{2,1}(k) \\ \mathbf{s}_{1,1}(k) \\ \hline \mathbf{s}_{2,1}^*(N-k+2) \\ \mathbf{s}_{1,1}^*(N-k+2) \end{bmatrix} \tag{67}$$

$$\tilde{\mathcal{Z}}_k^{(\mathrm{Al})} = \begin{bmatrix} \mathcal{Z}_k^{(\mathrm{Al})} \\ \hline \mathcal{Z}_{N-k+2}^{(\mathrm{Al})} \end{bmatrix} = \begin{bmatrix} \mathbf{z}_{1,1}(k) \\ \mathbf{z}_{1,2}^*(k) \\ \hline \mathbf{z}_{1,1}^*(N-k+2) \\ \mathbf{z}_{1,2}(N-k+2) \end{bmatrix}. \tag{68}$$

Then

$$\underbrace{\tilde{\mathcal{Z}}_k^{(\mathrm{Al})}}_{4\times 1} = \underbrace{\tilde{\boldsymbol{\mathcal{G}}}_k}_{4\times 4} \underbrace{\tilde{\mathcal{S}}_k^{(\mathrm{Al})}}_{4\times 1} + \underbrace{\tilde{\mathcal{V}}_k^{(\mathrm{Al})}}_{4\times 1} \tag{69}$$

with

$$\tilde{\boldsymbol{\mathcal{G}}}_k = \left[\begin{array}{c|c} \boldsymbol{\mathcal{G}}_{\mu,k} & \boldsymbol{\mathcal{G}}_{\nu,N-k+2} \\ \hline \boldsymbol{\mathcal{G}}_{\nu,k} & \boldsymbol{\mathcal{G}}_{\mu,N-k+2} \end{array}\right] \tag{70}$$

where

$$\boldsymbol{\mathcal{G}}_{\mu,k} = \begin{bmatrix} \mu_1\lambda_{1,2}(k) & \mu_1\lambda_{1,1}(k) \\ -\mu_1^*\lambda_{1,1}^*(k) & \mu_1^*\lambda_{1,2}^*(k) \end{bmatrix} \tag{71}$$

$$\boldsymbol{\mathcal{G}}_{\nu,k} = \begin{bmatrix} \nu_1^*\lambda_{1,2}(k) & \nu_1^*\lambda_{1,1}(k) \\ -\nu_1\lambda_{1,1}^*(k) & \nu_1\lambda_{1,2}^*(k) \end{bmatrix} \tag{72}$$

$$\boldsymbol{\mathcal{G}}_{\nu,N-k+2} = \begin{bmatrix} \nu_1\lambda_{1,2}^*(N-k+2) & \nu_1\lambda_{1,1}^*(N-k+2) \\ -\nu_1^*\lambda_{1,1}(N-k+2) & \nu_1^*\lambda_{1,2}(N-k+2) \end{bmatrix} \tag{73}$$

$$\boldsymbol{\mathcal{G}}_{\mu,N-k+2} = \begin{bmatrix} \mu_1^*\lambda_{1,2}^*(N-k+2) & \mu_1\lambda_{1,1}^*(N-k+2) \\ -\mu_1\lambda_{1,1}(N-k+2) & \mu_1\lambda_{1,2}(N-k+2) \end{bmatrix}. \tag{74}$$

Each of these submatrices satisfies the orthogonality condition in (66) with a different scaling factor. Note that the matrix $\tilde{\boldsymbol{\mathcal{G}}}_k$ in (70) would be block diagonal if $\nu_1 = 0$, i.e., if there were no IQ imbalances, in which case, (69) would reduce to two 2×2 decoupled systems, as in standard Alamouti decoding. The off-diagonal matrices in (70) are a result of the IQ imbalances. Therefore, we now need to deal with a 4×4 linear system of equations, as opposed to two decoupled 2×2 linear systems of equations. Still, the Alamouti structure of the submatrices in $\tilde{\boldsymbol{\mathcal{G}}}_k$ allows a computationally efficient implementation of the least-squares estimate of $\tilde{\mathcal{S}}_k^{(\mathrm{Al})}$ from $\tilde{\mathcal{Z}}_k^{(\mathrm{Al})}$ in (69), namely[3]

$$\widehat{\tilde{\mathcal{S}}}_k^{(\mathrm{Al})} = \left(\delta\mathbf{I} + \tilde{\boldsymbol{\mathcal{G}}}_k^*\tilde{\boldsymbol{\mathcal{G}}}_k\right)^{-1} \tilde{\boldsymbol{\mathcal{G}}}_k^* \tilde{\mathcal{Z}}_k^{(\mathrm{Al})} \tag{75}$$

Note that the term $\tilde{\boldsymbol{\mathcal{G}}}_k^*\tilde{\boldsymbol{\mathcal{G}}}_k$ has the following form:

$$\tilde{\boldsymbol{\mathcal{G}}}_k^*\tilde{\boldsymbol{\mathcal{G}}}_k = \begin{bmatrix} \mathbf{D}_1 & \mathbf{C}_1 \\ \mathbf{C}_2 & \mathbf{D}_2 \end{bmatrix} \tag{76}$$

where a regularization parameter $\delta > 0$ is used.

$$\begin{aligned} \mathbf{D}_1 &= \delta\mathbf{I} + \boldsymbol{\mathcal{G}}_{\mu,k}^*\boldsymbol{\mathcal{G}}_{\mu,k} + \boldsymbol{\mathcal{G}}_{\nu,k}^*\boldsymbol{\mathcal{G}}_{\nu,k} \\ &= \delta\mathbf{I} + (|\mu_1|^2 + |\nu_1|^2)(|\lambda_{1,1}(k)|^2 + |\lambda_{1,2}(k)|^2)\mathbf{I}_{2\times 2} \\ \mathbf{D}_2 &= \delta\mathbf{I} + \boldsymbol{\mathcal{G}}_{\nu,N-k+2}^*\boldsymbol{\mathcal{G}}_{\nu,N-k+2} + \boldsymbol{\mathcal{G}}_{\mu,N-k+2}^*\boldsymbol{\mathcal{G}}_{\mu,N-k+2} \\ &= \delta\mathbf{I} + (|\mu_1|^2 + |\nu_1|^2) \\ &\qquad \times (|\lambda_{1,1}(N-k+2)|^2 + |\lambda_{1,2}(N-k+2)|^2)\mathbf{I}_{2\times 2} \\ \mathbf{C}_1 &= \boldsymbol{\mathcal{G}}_{\mu,k}^*\boldsymbol{\mathcal{G}}_{\nu,N-k+2} + \boldsymbol{\mathcal{G}}_{\nu,k}^*\boldsymbol{\mathcal{G}}_{\mu,N-k+2} \\ \mathbf{C}_2 &= \boldsymbol{\mathcal{G}}_{\nu,N-k+2}^*\boldsymbol{\mathcal{G}}_{\mu,k} + \boldsymbol{\mathcal{G}}_{\mu,N-k+2}^*\boldsymbol{\mathcal{G}}_{\nu,k}. \end{aligned} \tag{77}$$

The matrices $\mathbf{D}_1$ and $\mathbf{D}_2$ are diagonal, whereas $\mathbf{C}_1$ and $\mathbf{C}_2$ are again 2×2 Alamouti structured matrices. This is because the product and summation of 2×2 Alamouti matrices is 2×2 Alamouti again. Furthermore, note that $\mathbf{C}_2 = \mathbf{C}_1^*$. A useful property of Alamouti matrices is that their inverses can be obtained by conjugate-transposing them. Now consider the following matrix inversion formula:

$$\begin{aligned} &\begin{bmatrix} \mathbf{D}_1 & \mathbf{C}_1 \\ \mathbf{C}_2 & \mathbf{D}_2 \end{bmatrix}^{-1} \\ &\quad = \begin{bmatrix} \boldsymbol{\Sigma}^{-1} & -\boldsymbol{\Sigma}^{-1}\mathbf{C}_1\mathbf{D}_2^{-1} \\ -\mathbf{D}_2^{-1}\mathbf{C}_2\boldsymbol{\Sigma}^{-1} & \mathbf{D}_2^{-1} + \mathbf{D}_2^{-1}\mathbf{C}_2\boldsymbol{\Sigma}^{-1}\mathbf{C}_1\mathbf{D}_2 \end{bmatrix} \end{aligned} \tag{78}$$

where

$$\boldsymbol{\Sigma} = \mathbf{D}_1 - \mathbf{C}_1\mathbf{D}_2^{-1}\mathbf{C}_2.$$

Let $\mathbf{D}_1 = d_1\mathbf{I}$ and $\mathbf{D}_2 = d_2\mathbf{I}$. Furthermore, $\mathbf{C}_1\mathbf{C}_2$ can be written as $d_3\mathbf{I}$, since $\mathbf{C}_1$ and $\mathbf{C}_2$ are Alamouti structured matrices and related through $\mathbf{C}_2 = \mathbf{C}_1^*$. Then

$$\boldsymbol{\Sigma} = \left(d_1 - \frac{d_3}{d_2}\right)\mathbf{I}$$

is diagonal. Thus, using the above formula to calculate the inverse of $\tilde{\boldsymbol{\mathcal{G}}}_k^*\tilde{\boldsymbol{\mathcal{G}}}_k$ in (76), one can see that all the terms in (78) are trivial to compute since all the matrices to be inverted are diagonal.

VI. Extension to Other Orthogonal Space-Time Block Codes (OSTBC)

We now show how the procedure of the previous section for Alamouti codes can be extended to any OSTBC [17]. More specifically, the procedure that led from (54) to (69) in the case of Alamouti codes will be extended to any orthogonal space-time block code. The derivations in this section are presented

[3]If desired, a regularization parameter may be added to (75).

for a system with a single receive antenna. In the context of orthogonal space-time block codes, the case of multiple receive antennas is a simple extension of the single receive antenna case. The following notation is adopted for the transmitted block of data $\boldsymbol{\mathcal{S}}_k^{(B)}$ in the case of orthogonal space-time block codes [18]:

$$\boldsymbol{\mathcal{S}}_k^{(B)} = \sum_{n=1}^{n_s} \left(\mathrm{Re}\left\{\mathbf{s}_n'(k)\right\}\mathbf{A}_n + j\mathrm{Im}\left\{\mathbf{s}_n'(k)\right\}\mathbf{B}_n\right) \tag{79}$$

where $\{\mathbf{A}_n, \mathbf{B}_n\}$ is a set of predefined $n_T \times p$ coding matrices and is known to both transmitter and receiver. Moreover, n_s denotes the number of independent symbols used to compose each transmitted block of data of size $(n_T \times p)$, and $\mathbf{s}_n'(k)$, $n = \{1, \ldots, n_s\}$ represents the set of independent symbols used to compose the transmitted block of data on tone k. Now, let us consider the system defined by (54) for a general $1 \times n_T$ orthogonal space-time block code. For a receiver without distortion, this system reduces to two decoupled systems of the form (with $\boldsymbol{\Pi}_\mu = 1$ and $\boldsymbol{\Pi}_\nu = 0$)

$$\underbrace{\boldsymbol{\mathcal{Z}}_k^{(B)}}_{1\times p} = \underbrace{\boldsymbol{\mathcal{H}}_k}_{1\times n_T}\underbrace{\boldsymbol{\mathcal{S}}_k^{(B)}}_{n_T\times p} + \underbrace{\boldsymbol{\mathcal{V}}_k^{(B)}}_{1\times p} \tag{80}$$

where, similar to (61) and (62), the channel matrix $\boldsymbol{\mathcal{H}}_k$ is given by

$$\boldsymbol{\mathcal{H}}_k = \left[\lambda_{1,n_T}(k) \quad \ldots \quad \lambda_{1,1}(k)\right]. \tag{81}$$

It is shown in [18] that for any OSTBC, the system (80) can be reorganized into an equivalent system of the form

$$\underbrace{\bar{\mathcal{Z}}_k}_{p\times 1} = \underbrace{\boldsymbol{\mathcal{F}}_k}_{p\times 2n_s}\underbrace{\bar{\mathcal{S}}_k}_{2n_s\times 1} + \underbrace{\bar{\mathcal{V}}_k}_{p\times 1} \tag{82}$$

where

$$\begin{aligned}\tilde{\mathcal{Z}}_k &= \mathrm{vec}\left(\boldsymbol{\mathcal{Z}}_k^{(B)}\right)\\ \bar{\mathcal{V}}_k &= \mathrm{vec}\left(\mathcal{V}_k^{(B)}\right)\end{aligned} \tag{83}$$

and

$$\bar{\mathcal{S}}_k = \begin{bmatrix}\mathrm{Re}\left\{\mathbf{s}_{n_s}'(k)\right\}\\ \vdots\\ \mathrm{Re}\left\{\mathbf{s}_1'(k)\right\}\\ \mathrm{Im}\left\{\mathbf{s}_{n_s}'(k)\right\}\\ \vdots\\ \mathrm{Im}\left\{\mathbf{s}_1'(k)\right\}\end{bmatrix}, \quad \boldsymbol{\mathcal{F}}_k = \begin{bmatrix}\mathrm{vec}^T(\boldsymbol{\mathcal{H}}_k\mathbf{A}_{n_s})\\ \vdots\\ \mathrm{vec}^T(\boldsymbol{\mathcal{H}}_k\mathbf{A}_1)\\ i\mathrm{vec}^T(\boldsymbol{\mathcal{H}}_k\mathbf{B}_{n_s})\\ \vdots\\ i\mathrm{vec}^T(\boldsymbol{\mathcal{H}}_k\mathbf{B}_1)\end{bmatrix}^T \tag{84}$$

where the notation in (79) is used, and $[\cdot]^T$ is the matrix transpose operation. The least-squares solution to the above problem is [18]

$$\hat{\bar{\mathcal{S}}}_k = \left(\mathrm{Re}\left\{\boldsymbol{\mathcal{F}}_k^*\boldsymbol{\mathcal{F}}_k\right\}\right)^{-1}\mathrm{Re}\left\{\boldsymbol{\mathcal{F}}_k^*\bar{\mathcal{Z}}_k\right\} \tag{85}$$

where the following orthogonality property holds (due to the orthogonality of the space-time block code):

$$\mathrm{Re}\left\{\boldsymbol{\mathcal{F}}_k^*\boldsymbol{\mathcal{F}}_k\right\} = \|\boldsymbol{\mathcal{H}}_k\|^2\mathbf{I} \tag{86}$$

where $\|\cdot\|$ is the Euclidean norm.

In the case of IQ imbalances, it can be verified by following the same argument that resulted in (69)–(74) that the system of equations (54) in the case of orthogonal space-time block codes can be reduced to

$$\underbrace{\tilde{\mathcal{Z}}_k}_{2p\times 1} = \underbrace{\tilde{\boldsymbol{\mathcal{F}}}_k}_{2p\times 4n_s}\underbrace{\tilde{\mathcal{S}}_k}_{4n_s\times 1} + \underbrace{\tilde{\mathcal{V}}_k}_{2p\times 1} \tag{87}$$

with

$$\tilde{\boldsymbol{\mathcal{F}}}_k = \left[\begin{array}{c|c}\boldsymbol{\mathcal{F}}_{\mu,k} & \boldsymbol{\mathcal{F}}_{\nu,N-k+2}\\ \hline \boldsymbol{\mathcal{F}}_{\nu,k} & \boldsymbol{\mathcal{F}}_{\mu,N-k+2}\end{array}\right] \tag{88}$$

where $\boldsymbol{\mathcal{F}}_{\mu,k}$, $\boldsymbol{\mathcal{F}}_{\nu,N-k+2}$, $\boldsymbol{\mathcal{F}}_{\nu,k}$, and $\boldsymbol{\mathcal{F}}_{\mu,N-k+2}$ are defined by the channel matrices $\boldsymbol{\Pi}_\mu\boldsymbol{\mathcal{H}}_k$, $\boldsymbol{\Pi}_\nu\boldsymbol{\mathcal{H}}_{N-k+2}$, $\boldsymbol{\Pi}_\nu^*\boldsymbol{\mathcal{H}}_k$, and $\boldsymbol{\Pi}_\mu^*\boldsymbol{\mathcal{H}}_{N-k+2}$ in (54), respectively, in a manner similar to how the matrix $\boldsymbol{\mathcal{F}}_k$ in (84) was defined from $\boldsymbol{\mathcal{H}}_k$. Furthermore

$$\begin{aligned}\tilde{\mathcal{Z}}_k &= \left[\begin{array}{c}\tilde{\mathcal{Z}}_k\\ \hline \bar{\mathcal{Z}}_{N-k+2}\end{array}\right]\\ \tilde{\mathcal{V}}_k &= \left[\begin{array}{c}\tilde{\mathcal{V}}_k\\ \hline \bar{\mathcal{V}}_{N-k+2}\end{array}\right]\\ \tilde{\mathcal{S}}_k &= \left[\begin{array}{c}\tilde{\mathcal{S}}_k\\ \hline \bar{\mathcal{S}}_{N-k+2}\end{array}\right]\end{aligned} \tag{89}$$

where, based on the structure of (54)

$$\begin{aligned}\bar{\mathcal{Z}}_k &= \mathrm{vec}\left(\boldsymbol{\mathcal{Z}}_k^{(B)}\right)\\ \bar{\mathcal{Z}}_{N-k+2} &= \mathrm{vec}\left(\boldsymbol{\mathcal{Z}}_{N-k+2}^{(B)}\right)\\ \bar{\mathcal{V}}_k &= \mathrm{vec}\left(\boldsymbol{\mathcal{V}}_k^{(B)}\right)\\ \bar{\mathcal{V}}_{N-k+2} &= \mathrm{vec}\left(\boldsymbol{\mathcal{V}}_{N-k+2}^{(B)}\right)\end{aligned} \tag{90}$$

and $\bar{\mathcal{S}}_k$ and $\bar{\mathcal{S}}_{N-k+2}$ are defined from $\boldsymbol{\mathcal{S}}_k^{(B)}$ and $\boldsymbol{\mathcal{S}}_{N-k+2}^{(B)}$, respectively, in a manner similar to (84).

It can be seen that the submatrices in (88) satisfy the orthogonality conditions

$$\begin{aligned}\mathrm{Re}\{\boldsymbol{\mathcal{F}}_{\mu,k}^*\boldsymbol{\mathcal{F}}_{\mu,k}\} &= |\mu_1|^2\|\boldsymbol{\mathcal{H}}_k\|^2\mathbf{I}\\ \mathrm{Re}\{\boldsymbol{\mathcal{F}}_{\nu,k}^*\boldsymbol{\mathcal{F}}_{\nu,k}\} &= |\nu_1|^2\|\boldsymbol{\mathcal{H}}_k\|^2\mathbf{I}\\ \mathrm{Re}\{\boldsymbol{\mathcal{F}}_{\mu,N-k+2}^*\boldsymbol{\mathcal{F}}_{\mu,N-k+2}\} &= |\mu_1|^2\|\boldsymbol{\mathcal{H}}_{N-k+2}\|^2\mathbf{I}\\ \mathrm{Re}\{\boldsymbol{\mathcal{F}}_{\nu,N-k+2}^*\boldsymbol{\mathcal{F}}_{\nu,N-k+2}\} &= |\nu_1|^2\|\boldsymbol{\mathcal{H}}_{N-k+2}\|^2\mathbf{I}\end{aligned} \tag{91}$$

where $\boldsymbol{\Pi}_\mu$ and $\boldsymbol{\Pi}_\nu$ are reduced to μ_1 and ν_1, respectively, for a $1 \times n_T$ system.

The least-squares estimate of $\tilde{\mathcal{S}}_k$ from (87) is then given by[4]

$$\hat{\tilde{\mathcal{S}}}_k = \left(\text{Re}\left\{\tilde{\boldsymbol{\mathcal{F}}}_k^* \tilde{\boldsymbol{\mathcal{F}}}_k\right\}\right)^{-1} \text{Re}\left\{\tilde{\boldsymbol{\mathcal{F}}}_k^* \tilde{\mathcal{Z}}_k\right\} \tag{92}$$

where, in a manner similar to the previous section [see (76)], the term $\text{Re}\left\{\tilde{\boldsymbol{\mathcal{F}}}_k^* \tilde{\boldsymbol{\mathcal{F}}}_k\right\}$ has the following form:

$$\text{Re}\left\{\tilde{\boldsymbol{\mathcal{F}}}_k^* \tilde{\boldsymbol{\mathcal{F}}}_k\right\} = \begin{bmatrix} \mathbf{D}_1 & \mathbf{C}_1 \\ \mathbf{C}_2 & \mathbf{D}_2 \end{bmatrix}$$

with

$$\begin{aligned}
\mathbf{D}_1 &= \text{Re}\left\{\boldsymbol{\mathcal{F}}_{\mu,k}^* \boldsymbol{\mathcal{F}}_{\mu,k}\right\} + \text{Re}\left\{\boldsymbol{\mathcal{F}}_{\nu,k}^* \boldsymbol{\mathcal{F}}_{\nu,k}\right\} \\
&= (|\mu_1|^2 + |\nu_1|^2)\|\boldsymbol{\mathcal{H}}_k\|^2 \mathbf{I} \\
\mathbf{D}_2 &= \text{Re}\left\{\boldsymbol{\mathcal{F}}_{\mu,N-k+2}^* \boldsymbol{\mathcal{F}}_{\mu,N-k+2}\right\} \\
&\quad + \text{Re}\left\{\boldsymbol{\mathcal{F}}_{\nu,N-k+2}^* \boldsymbol{\mathcal{F}}_{\nu,N-k+2}\right\} \\
&= (|\mu_1|^2 + |\nu_1|^2)\|\boldsymbol{\mathcal{H}}_{N-k+2}\|^2 \mathbf{I} \\
\mathbf{C}_1 &= \text{Re}\left\{\boldsymbol{\mathcal{F}}_{\mu,k}^* \boldsymbol{\mathcal{F}}_{\nu,N-k+2}\right\} + \text{Re}\left\{\boldsymbol{\mathcal{F}}_{\nu,k}^* \boldsymbol{\mathcal{F}}_{\mu,N-k+2}\right\} \\
\mathbf{C}_2 &= \text{Re}\left\{\boldsymbol{\mathcal{F}}_{\nu,N-k+2}^* \boldsymbol{\mathcal{F}}_{\mu,k}\right\} + \text{Re}\left\{\boldsymbol{\mathcal{F}}_{\mu,N-k+2}^* \boldsymbol{\mathcal{F}}_{\nu,k}\right\}.
\end{aligned} \tag{93}$$

VII. Further Issues

A. Frequency-Flat versus Frequency-Selective IQ Imbalances

We now briefly discuss the frequency selectivity of the IQ imbalances and its effect on the receiver architectures presented in this paper. The distortion parameters μ_m and ν_m, $m = \{1, \ldots, n_R\}$ have been considered constant throughout the derivations. By that, we mean that the μ_m and ν_m defined by (2) are assumed to be frequency independent since the physical mismatches θ and α in (2) are considered to be so. An important consequence of this assumption is that the $(n_R \times n_T)$ channel matrices defined by (35) use the same $\{\mu_1, \ldots, \mu_{n_R}\}$ and $\{\nu_1, \ldots, \nu_{n_R}\}$ parameters for all the tones $k = \{2, \ldots, N/2\}$, i.e., μ_m and ν_m are independent of the tone index k. This is only valid if the physical imbalances are constant over the frequency band of operation. This is a valid assumption if the OFDM signal bandwidth is relatively small compared with the carrier frequency [4]. The impact of frequency dependency of IQ imbalances on the compensation schemes in the SISO case is discussed in greater detail in , and a similar argument holds for the MIMO case. For systems with higher bandwidths, this assumption is no longer realistic, and the imbalances may vary with frequency. Under such conditions, a frequency-selective IQ imbalance model is to be used. For frequency-selective imbalances, the system of equations governed by (35) can be modified by using frequency-dependent μ_m and ν_m, $m = \{1, \ldots, n_R\}$ parameters. In other words, for the kth tone, the distortion parameters in the equations should be considered as $\mu_m(k)$ and $\nu_m(k)$. This modification will not affect the compensation schemes presented in the paper since they did not use the k-independency of μ_m and ν_m in the first place.

[4]This is because

$$\hat{\bar{\mathcal{S}}}_k = \arg\min_{\bar{\mathcal{S}}_k} \|\bar{\mathcal{Z}}_k - \bar{\boldsymbol{\mathcal{F}}}_k \bar{\mathcal{S}}_k\|^2.$$

It can be verified that

$$\begin{aligned}
&\|\bar{\mathcal{Z}}_k - \bar{\boldsymbol{\mathcal{F}}}_k \bar{\mathcal{S}}_k\|^2 \\
&\quad = \left(\bar{\mathcal{S}}_k - \left(\text{Re}\left\{\bar{\boldsymbol{\mathcal{F}}}_k^* \bar{\boldsymbol{\mathcal{F}}}_k\right\}\right)^{-1} \text{Re}\left\{\bar{\boldsymbol{\mathcal{F}}}_k^* \bar{\mathcal{Z}}_k\right\}\right)^* \text{Re}\left\{\bar{\boldsymbol{\mathcal{F}}}_k^* \bar{\boldsymbol{\mathcal{F}}}_k\right\} \\
&\qquad \times \left(\bar{\mathcal{S}}_k - \left(\text{Re}\left\{\bar{\boldsymbol{\mathcal{F}}}_k^* \bar{\boldsymbol{\mathcal{F}}}_k\right\}\right)^{-1} \text{Re}\left\{\bar{\boldsymbol{\mathcal{F}}}_k^* \bar{\mathcal{Z}}_k\right\}\right) + \text{const.}
\end{aligned}$$

where we used the fact that

$$\|\bar{\boldsymbol{\mathcal{F}}}_k \bar{\mathcal{S}}_k\|^2 = \bar{\mathcal{S}}_k^* \text{Re}\left\{\bar{\boldsymbol{\mathcal{F}}}_k^* \bar{\boldsymbol{\mathcal{F}}}_k\right\} \bar{\mathcal{S}}_k.$$

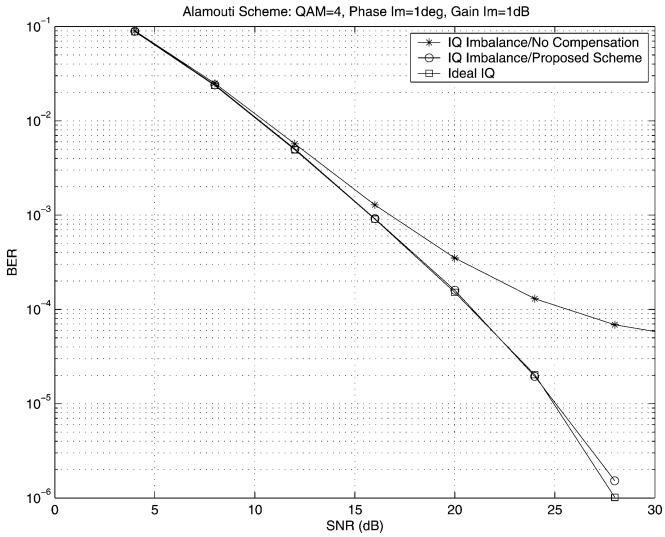

Fig. 5. BER versus SNR for an OFDM system with Alamouti space-time coding. The simulation parameters are phase mismatch of $\theta = 1^\circ$, amplitude mismatch of $\alpha = 1$ dB [see (2)], and 4QAM constellation.

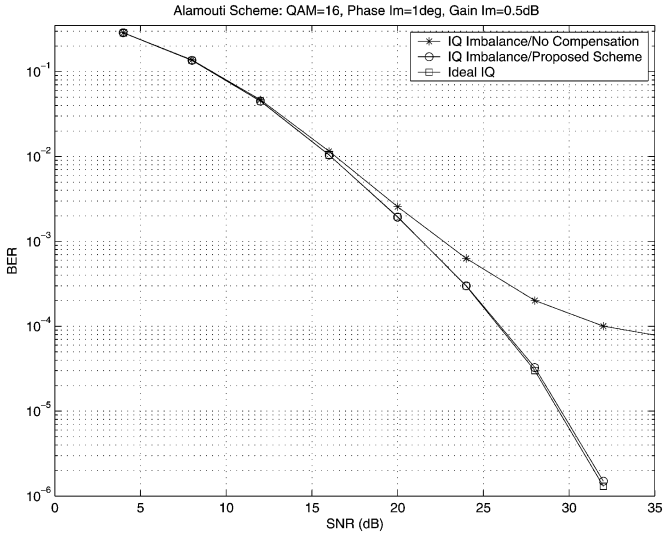

Fig. 6. BER versus SNR for an OFDM system with Alamouti space-time coding. The simulation parameters are phase mismatch of $\theta = 1^\circ$, amplitude mismatch of $\alpha = 0.5$ dB [see (2)], and 16QAM constellation.

B. Joint Channel and Distortion Parameter Estimation

The problem of estimating the channel/distortion parameters $\{\lambda_{m,l}(k), \mu_m, \nu_m\}$ needed at the receiver for data recovery is not discussed in this paper. It is useful to realize that in the presence of IQ imbalances, the channel and distortion parameters are required for data recovery in a joint manner [see (77)]. In other

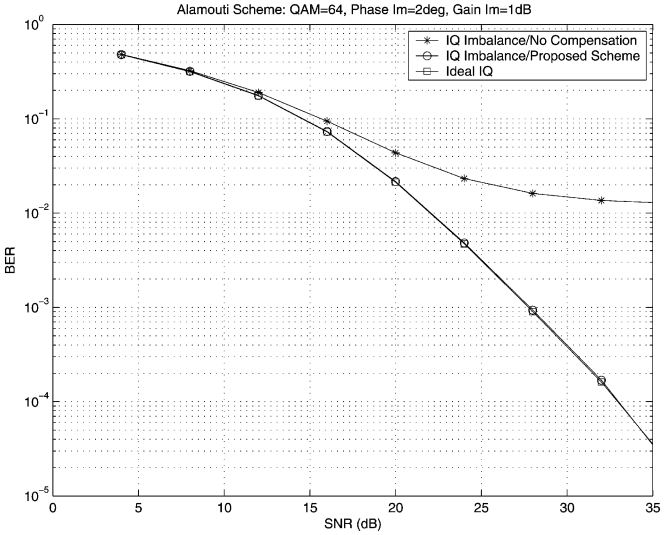

Fig. 7. BER versus SNR for an OFDM system with Alamouti space-time coding. The simulation parameters are phase mismatch of $\theta = 2^\circ$, amplitude mismatch of $\alpha = 1$ dB [see (2)], and 64QAM constellation.

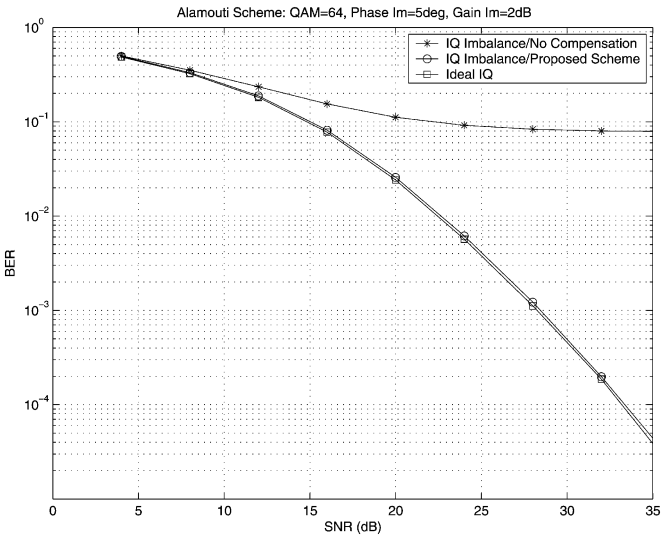

Fig. 8. BER versus SNR for an OFDM system with Alamouti space-time coding. The simulation parameters are phase mismatch of $\theta = 5^\circ$, amplitude mismatch of $\alpha = 2$ dB [see (2)], and 64QAM constellation.

words, the channel and distortion parameters are not required separately at the receiver, but a combination of them is used in the proposed receiver algorithms. For instance, in the Alamouti case, the scalar factor of the diagonal matrix $\mathbf{D}_1$ in (77) is the sum of the squared values of the first-column elements in $\boldsymbol{\mathcal{G}}_{\mu,k}$ and $\boldsymbol{\mathcal{G}}_{\nu,k}$. A joint channel and distortion estimation task at the receiver is then equivalent to estimating the matrix $\tilde{\boldsymbol{\mathcal{G}}}_k$ defined by (70). The input–output system given by (69) can be used to estimate $\tilde{\boldsymbol{\mathcal{G}}}_k$ from the received data $\tilde{\mathcal{Z}}_k^{(\mathrm{AI})}$, possibly by transmitting training data. Standard MIMO channel estimation algorithms can be applied here as well, since (69) essentially defines a MIMO problem with dimension 4×4. Similar to the data recovery algorithms, the structure of the system given by (69) can be exploited to derive efficient channel estimation algorithms. Addressing the channel estimation problem is beyond the scope

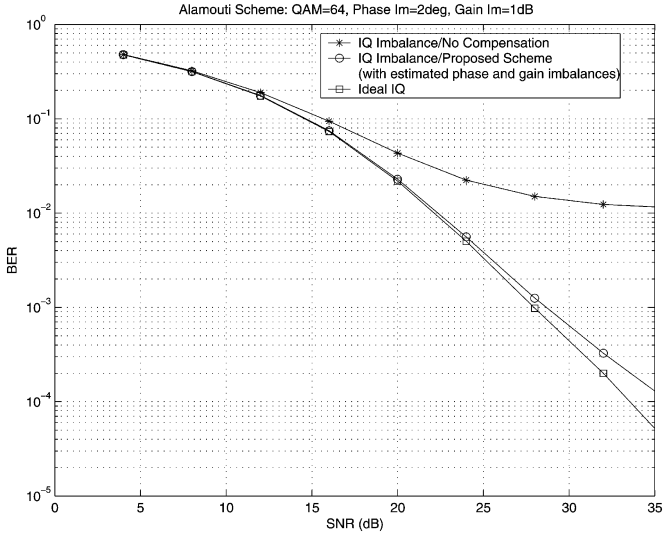

Fig. 9. BER versus SNR for an OFDM system with Alamouti space-time coding. The proposed scheme is using estimates of the distortion parameters ($\theta = 1.8^\circ$ and $\alpha = 0.8$ dB) instead of the exact distortion parameters ($\theta = 2^\circ$ and $\alpha = 1$ dB).

of this paper. However, some efficient channel/distortion estimation schemes for the SISO case can be found in . The schemes presented there can be used as a starting point for channel/distortion estimation in the MIMO case.

VIII. Simulation Results

A typical OFDM system with space-time coding is simulated to evaluate and compare the performance of the proposed schemes. In the simulations, the Alamouti scheme is applied on a (2×1)-OFDM system, as was described in Section V. The parameters used in the simulation are as follows: OFDM symbol length of $N = 64$, cyclic prefix of $P = 16$, and channel length of $(L + 1) = 4$. The channel taps corresponding to two transmit antennas are chosen independently with complex Gaussian distribution. In Figs. 5–8, "Ideal IQ" legend refers to a receiver with perfect IQ branches and perfect channel knowledge. The "IQ Imbalance/No Compensation" refers to a receiver with IQ imbalances without any compensation scheme. Finally, "IQ Imbalance/Proposed Scheme" refers to the receiver architecture proposed in Section V. Fig. 9 demonstrates how sensitive the proposed algorithm is to errors in the estimates of phase and amplitude imbalances. In this figure, the proposed algorithm uses estimates of the distortion parameters ($\theta = 1.8^\circ$ and $\alpha = 0.8$ dB) instead of the exact distortion parameters ($\theta = 2^\circ$ and $\alpha = 1$ dB). The proposed scheme results in an acceptable performance, even with such errors in the distortion parameters estimates.

IX. Conclusions

The simulation results show that the achievable BER versus SNR in a system assuming ideal IQ branches can be severely limited by IQ imbalances. Combating the IQ imbalances in the digital domain has many advantages over the analog domain in terms of overall cost and complexity. The digital domain approach is motivated by the fact that the analog domain schemes

are expensive in terms of area (cost) and power and are unable to completely remove such distortions. In this paper, receiver algorithms were derived for Alamouti-coded OFDM systems and were extended to other orthogonal space-time block-coded OFDM systems. In both cases, the receiver complexity was reduced by exploiting the orthogonal structure of the codes. The simulation results showed that the proposed receiver achieves a BER curve that is close to that of a system with ideal IQ branches. In the case of Alamouti codes, this improvement is achieved with a complexity that is close to that of a standard receiver with ideal IQ branches.

REFERENCES

[1] A. Tarighat and A. H. Sayed, "Space-time coding in MISO-OFDM systems with implementation impairments," in *Proc. Third IEEE Sensor Array Multichannel Signal Process. Workshop*, Barcelona, Spain, Jul. 2004.

[2] M. J. M. Pelgrom, A. C. J. Duinmaijer, and A. P. G. Welbers, "Matching properties of MOS transistors," *IEEE J. Solid-State Circuits*, vol. 24, no. 5, pp. 1433–1439, Oct. 1989.

[3] A. Tarighat, R. Bagheri, and A. H. Sayed, "Compensation schemes and performance analysis of IQ inhabitants in OFDM receivers," *IEEE Trans. Signal Process.*, vol. 53, no. 8, pp. 3257–3268, Aug. 2005.

[4] B. Razavi, *RF Microelectronics*. Englewood Cliffs, NJ: Prentice-Hall, 1998.

[5] A. A. Abidi, "Direct-conversion radio transceivers for digital communications," *IEEE J. Solid-State Circuits*, vol. 30, no. 12, pp. 1399–1410, Dec. 1995.

[6] Z. Pengfei, N. Thai, C. Lam, D. Gambetta, C. Soorapanth, C. Baohong, S. Hart, I. Sever, T. Bourdi, A. Tham, and B. Razavi, "A direct conversion CMOS transceiver for IEEE 802.11a WLANs," in *IEEE Int. Solid-State Circuits Conf. Dig. Tech. Papers*, vol. 1, Feb. 2003, pp. 354–498.

[7] A. Baier, "Quadrature mixer imbalances in digital TDMA mobile radio receivers," in *Proc. Int. Zurich Seminar Digital Commun., Electron. Circuits Syst. Commun.*, Mar. 1990, pp. 147–162.

[8] C. L. Liu, "Impacts of I/Q imbalance on QPSK-OFDM-QAM detection," *IEEE Trans. Consumer Electron.*, vol. 44, no. 3, pp. 984–989, Aug. 1998.

[9] A. Schuchert, R. Hasholzner, and P. Antoine, "A novel IQ imbalance compensation scheme for the reception of OFDM signals," *IEEE Trans. Consumer Electron.*, vol. 47, no. 3, pp. 313–318, Aug. 2001.

[10] S. Fouladifard and H. Shafiee, "Frequency offset estimation in OFDM systems in presence of IQ imbalance," in *Proc. Int. Conf. Commun.*, Anchorage, AK, May 2003, pp. 2071–2075.

[11] J. Tubbax, B. Come, L. V. der Perre, S. Donnay, M. Engels, M. Moonen, and H. D. Man, "Joint compensation of IQ imbalance and frequency offset in OFDM systems," in *Proc. Radio Wireless Conf.*, Boston, MA, Aug. 2003, pp. 39–42.

[12] A. Tarighat and A. H. Sayed, "An optimum OFDM receiver exploiting cyclic prefix for improved data estimation," in *Proc. IEEE Int. Conf. Acoust., Speech, Signal Process.*, vol. 4, Hong Kong, Apr. 2003, pp. 217–220.

[13] G. G. Raleigh and V. K. Jones, "Multivariate modulation and coding for wireless communications," *IEEE J. Sel. Areas Commun.*, vol. 17, no. 5, pp. 851–866, May 1999.

[14] G. J. Foschini, "Layered space-time architecture for wireless communication in a fading environment when using multiple antennas," *Bell Labs Tech. J.*, vol. 1, pp. 41–59, 1996.

[15] G. J. Foschini and M. J. Gans, "On limits of wireless communications in a fading environment when using multiple antennas," *Wireless Pers. Commun.*, vol. 6, pp. 311–335, Mar. 1998.

[16] S. M. Alamouti, "A simple transmit diversity technique for wireless communications," *IEEE J. Sel. Areas Commun.*, vol. 16, no. 8, pp. 1451–1458, Oct. 1998.

[17] V. Tarokh, H. Jafrakhani, and A. R. Calderbank, "Space-time block codes from orthogonal designs," *IEEE Trans. Inf. Theory*, vol. 45, no. 5, pp. 1456–1467, Jul. 1999.

[18] E. G. Larsson and P. Stoica, "Mean-square-error optimality of orthogonal space-time block codes," *IEEE Signal Process. Lett.*, vol. 10, no. 11, pp. 327–330, Nov. 2003.

Alireza Tarighat (S'00) received the B.Sc. degree in electrical engineering from Sharif University of Technology, Tehran, Iran, in 1998 and the M.Sc. degree in electrical engineering from the University of California, Los Angeles (UCLA), in 2001, with emphasis on integrated circuits and systems. Since April 2002, he has been pursuing the Ph.D. degree in electrical engineering at UCLA.

During the summer of 2000, he was with Broadcom, El Segundo, CA, where he worked on designing IEEE 802.11a transceivers. From 2001 to 2002, he was with Innovics Wireless, Los Angeles, as a Senior Design Engineer, working on ASIC implementation of advanced antenna diversity and rake processing for 3G WCDMA mobile terminals. His research focuses on signal processing techniques for communications, including MIMO OFDM receiver design, multiuser MIMO communications, and experimental wireless systems.

Mr. Tarighat received the Gold Medal of the National Physics Olympiad, Iran, in 1993 and the Honorable Mention Diploma of the 25th International Physics Olympiad, Beijing, China, in 1994.

Ali H. Sayed (F'01) received the Ph.D. degree in electrical engineering in 1992 from Stanford University, Stanford, CA.

He is Professor and Chairman of electrical engineering at the University of California, Los Angeles. He is also the Principal Investigator of the UCLA Adaptive Systems Laboratory (www.ee.ucla.edu/asl). He has over 200 journal and conference publications, is the author of the textbook *Fundamentals of Adaptive Filtering* (New York: Wiley, 2003), is coauthor of the research monograph *Indefinite Quadratic Estimation and Control* (Philadelphia, PA: SIAM, 1999) and of the graduate-level textbook *Linear Estimation* (Englewood Cliffs, NJ: Prentice-Hall, 2000). He is also co-editor of the volume *Fast Reliable Algorithms for Matrices with Structure* (Philadelphia, PA: SIAM, 1999). He has contributed several articles to engineering and mathematical encyclopedias and handbooks and has served on the program committees of several international meetings. He has also consulted with industry in the areas of adaptive filtering, adaptive equalization, and echo cancellation. His research interests span several areas, including adaptive and statistical signal processing, filtering and estimation theories, signal processing for communications, interplays between signal processing and control methodologies, system theory, and fast algorithms for large-scale problems.

Dr. Sayed is recipient of the 1996 IEEE Donald G. Fink Award, a 2002 Best Paper Award from the IEEE Signal Processing Society, the 2003 Kuwait Prize in Basic Science, the 2005 Frederick E. Terman Award, and co-author of two Best Student Paper awards at international meetings. He is also a member of the technical committees on Signal Processing Theory and Methods (SPTM) and on Signal Processing for Communications (SPCOM), both of the IEEE Signal Processing Society. He is a member of the editorial board of the IEEE SIGNAL PROCESSING MAGAZINE. He has also served twice as Associate Editor of the IEEE TRANSACTIONS ON SIGNAL PROCESSING, of which he is now serving as Editor-in-Chief. He is serving as General Chairman of ICASSP 2008.